Reliability Engineering and System Safety 251 (2024) 110336

Contents lists available at ScienceDirect

Reliability Engineering and System Safety

journal homepage: www.elsevier.com/locate/ress

A framework to analyse the probability of accidental hull girder failure considering advanced corrosion degradation for risk-based ship design

Krzysztof Woloszyk [a,*], Floris Goerlandt [b], Jakub Montewka [a]

[a] Institute of Naval Architecture, Gdansk University of Technology, Narutowicza 11/12 st., Gdansk, 80-233, Poland
[b] Maritime Risk and Safety Research Group, Department of Industrial Engineering, Dalhousie University, 5269 Morris Street, Halifax, NS B3H 4R2, Canada

ARTICLE INFO

Keywords:
Ship structures
Ultimate strength
Reliability
Risk-based ship design
Maritime accidents
Maritime safety

ABSTRACT

Ship's hull girder failure could result from maritime accident that can cause human life loss, environmental disaster, and major economic impacts. In risk-based ship design paradigm, accounting for rare phenomena (e.g. ship-ship collision or grounding) is important to provide safe and durable structure. In-service corrosion-induced hull degradation should be considered at the design stage, as it can significantly affect structural strength. The current study presents a novel framework to estimate the probability of ship hull girder failure, accounting for novel corrosion modelling techniques and accidental damage. The associated uncertainties are considered using statistical sampling from evidence-based distributions. A state-of-the-art deterministic model for ultimate strength calculation is applied using Monte Carlo simulation approach, resulting in the probability of hull failure through a reliability assessment. Wave and still-water bending moments are considered random variables. Two case studies of tanker ships with varying sizes are executed to show the applicability of the proposed framework. The results indicate that proper consideration of corrosion is of high importance, as ageing can significantly increase the probability of failure if accidental damage happens. Therefore, whereas future research and model refinement are discussed, the presented framework can serve for risk-based ship design tool and assess existing structures' safety.

1. Introduction

Many hazards can threaten the integrity of ships and offshore structures, necessitating a focus on the safety of ship designs. Risk-based ship design aims to consider the influence of various hazards on the design stage [1,2]. Ship collisions and groundings are widely recognized as major accident types in maritime transportation [3]. Although the frequency of serious ship accidents has significantly decreased over the past decades, ship collision and grounding accidents still regularly occur, and their potential for severe consequences is still considerable [4,5]. Those consequences can include high financial costs, loss of life and significant ecological impacts [6,7]. Several frameworks and risk analyses have been proposed to reduce the risks of those hazards. Focusing on ship design and operation, mitigation measures can lower the probability of accident occurrence [8] and/or reduce the severity of consequences should an accident occur [9]. On a wider level, further risk mitigation can be achieved through improved preparedness and response risk management and related decision-support tools [10,11].

Significant work has been dedicated to develop real-time approaches to estimate collision probability in ongoing operations, aimed at reducing the occurrence of accidents through improved decision-making for ship officers or Vessel Traffic Service (VTS) operators, see e.g. [12,13] for reviews. Closely related work has been dedicated to proposing methods for analysing collision risks in sea and waterway areas, aimed at area-based management of marine spaces, see e.g. [14,15] for reviews. Very recently, some works were dedicated to supporting hazard identification of autonomous vessels [16–18]. The framework for ship abnormal behaviour detection and classification based on AIS data was proposed in [19]. Other risk analysis approaches have been presented to support decisions on reducing the probability of ship collision accident occurrence through improvements at the ship design stage [20,21], or focus on managerial decision-making concerning the reduction of human and organizational errors in collision avoidance processes [22,23]. Similar work has been dedicated to grounding accidents, for instance, to assess real-time operational risk of grounding [24], to understand and mitigate human and organizational factors in groundings [25], and to develop ship contingency plans in case a grounding occurs [26]. However, for complex socio-technical systems, there is a strong consensus that attaining a "zero-accident" state is unrealistic. Hence, an important research area is to mitigate accident

* Corresponding author.
E-mail address: krzysztof.woloszyk@pg.edu.pl (K. Woloszyk).

https://doi.org/10.1016/j.ress.2024.110336
Received 5 April 2024; Received in revised form 28 June 2024; Accepted 7 July 2024
Available online 10 July 2024
0951-8320/

consequences, especially when the anticipated mitigation measures can be shown to have a high certainty of being effective [27].

Significant research efforts have also been dedicated to estimating the consequences of maritime accidents. Those includes loss of life (e.g. due to flooding) [28–30], loss of ship (including cargo) [31], and possible environmental pollution [32,33]. In [33], it was shown that consequences could be considered in a wider sense, having short-, medium- and long-term economic and socio-cultural impact. The aforementioned are usually the final and most prominent indicators of maritime accident outcomes, which could be useful from the perspective of insurance companies, stakeholders and society. However, what is most important from the designer's perspective should be rather associated with transient physical phenomena, which are the bridge between maritime accidents (e.g. collision) with consequences indicators (e.g. loss of ship). As suggested in [34], the criteria for risk-based ship design could be defined as the multiplication of the probability of accident occurrence with a probability of hull structural failure given the accident happened and consequences given structural failure. The consequences could be further expressed by the number of oil spills or the cost incurred by oil spills [35] for tanker ships. In the current work, the focus is on the probability of hull structural failure, given that an accident happened.

A comprehensive literature review regarding models to estimate the influence of ship-ship collisions in view of ship structure performance is given by [36]. Recently, advanced FE simulations were employed to analyse the structural behaviour of ships under collision or grounding [37,38]. However, the FE simulations of that scale are time-consuming and require significant modelling effort, which can be problematic in the design stage. A possible way to address this problem is to use a so-called super-FE method as presented for ship collisions by [39]. Some of the proposed models have also been applied in the context of risk-based ship design frameworks and/or for optimization of hull design, see, e.g. [35,40,41]. Depending on the ship type, damage consequence models were further coupled with models for further consequences of the collision or grounding, e.g., stability and flooding for passenger's vessels [29,42], and oil spill for cargo vessels and oil tankers [43–45]. Models for ship collisions have accounted for several important phenomena, including the deformability of the impacting bow [46], structural design of the impacted hull [47], the influence of hydrodynamic loads including sloshing on energy dissipation [48], the influence of compressive ice on energy absorption in bow-aft collisions [49], and recently configuration between struck and striking ship [50]. A comprehensive review of the state-of-the-art in collision and grounding modelling is provided in [3,36].

Despite the importance of ship age both as a contributing factor for the occurrence of accidents [51], as well as a compounding factor leading to lower structural strength [52], very little focus has been given to the influence of ageing mechanisms on collision-induced hull damage, with even less focus on the related probability of hull girder failure. Some limited studies on that topic include an analysis of structural crashworthiness of a corroded hull in stranding [53], and ultimate strength of tanker ship given collision damage [37]. In the latter, a simplified corrosion model was adopted, forming a good basis for further studies on that topic. However, there is no systematic understanding of the significance of ageing effects on the ensuing probability of hull girder failure. This will be especially dangerous for aged vessels. As shown in [54,55], the number of sunk vessels in the Black Sea alone is determined to be several per year, with the authors finding a clear correlation between ship's age and number of accidents. This is also consistent with the report presented by [56], showing that for older bulk carriers risk of serious consequences of accidents increases. Thus, it is of great importance to properly consider ageing effects in accidental limit states such as collision or grounding, and in estimating the probability of hull failure. Structural reliability analysis has been used for similar purposes [57–62].

The aim of this article is to propose a novel framework for the evaluation of the probability of hull girder failure, accounting for both corrosion degradation effects and accidental damage, see Section 2. This is considered as a probability of exceedance of the ultimate strength of the hull girder in view of associated uncertainties. When the ultimate strength is exceeded, the ship cross-section cannot carry more load, which results in the failure of the entire hull girder, i.e. "breaking" of the ship hull in two parts [63]. This could lead to major consequences, associated with the loss of the entire ship and a major oil spill from the cargo holds in an area where the collapse occurred (i.e. midship section). The main scientific advancement is the assessment of the effect of corrosion degradation on this probability when non-uniform thinning of structural elements on a local scale is considered as an ageing mechanism, which is discussed in Section 2.2. Notably, such an advanced approach for corrosion degradation modelling has to date not been accounted for in assessing the reliability of the ship's hull girder. This is achieved by introducing a corrosion correction factor to the progressive collapse modelling approach, accounting for uncertainty about this factor (see Section 2.3) and for the spatially random occurrence of thickness reduction within the ship's cross-section. The damage due to either collision or grounding is also considered a random variable (see Section 2.1). The ultimate strength probability distribution is determined with Monte Carlo simulations, to account for the uncertainties about the input conditions, resulting in a probabilistic ship design framework. Further, the probability of failure of the hull girder failure is estimated using a reliability analysis approach (see Section 2.4). Finally, the results are presented for two case studies for tanker vessels in sagging and hogging conditions, see Section 3, additionally presenting sensitivity analyses regarding how the damage extent and corrosion degradation are modelled. A discussion is provided in Section 4, whereas conclusions from the presented work are drawn in Section 5.

2. Methodology

The framework's very initial concept was presented in [64] where one deterministic damage extent due to ship-ship collision was analysed, showing that simultaneous consideration of corrosion degradation and accidental damage due to collision could result in a significantly increased probability of hull girder failure. Compared to that stage, there were several major improvements done in the current work, including:

- The additional case study of a grounding accident was considered in the framework, and damage extent was considered of a probabilistic nature;
- The algorithm to calculate the ultimate strength did not initially consider the rotation of the neutral axis, which should be taken into consideration due to the asymmetry of a damaged cross-section [65]. This was included in the current framework;
- The uncertainty due to the material strength decrease and local thickness non-uniformity due to corrosion degradation was additionally considered since it is well-known that corrosion has a negative effect on steel strength and brings additional uncertainty in ultimate strength prediction [66,67];
- The corrosion degradation level was considered non-uniformly distributed within the cross-section of the ship's hull in the current framework and not uniformly distributed, since it could have an impact on the structural response of the hull girder [68];
- In the reliability analysis, still water loads were considered for the damaged hull since several studies showed that there could be differences with comparison to still water loads for the intact hull [69,70], as considered in initial concept;
- Additional case study for a Handysize tanker was considered along with VLCC analysed previously to see the impact of ship size on the results.

The framework presented here for assessment of the probability of failure of hull girder, considering accidental damage and corrosion effects, presented in Fig. 1, aims to cover those improvements.

The presented framework could serve for risk-based ship design. The risk (which will be our design parameter) could be defined similarly as suggested in [34]:

$$R = P_{a|enc} \cdot P_{hf|a} \cdot C_{hf} \quad (1)$$

where $P_{a|enc}$ will the probability of accident (collision or grounding) given an encounter, $P_{hf|a}$ will be the probability of hull girder failure given an accident and C_{hf} will be the consequences of hull girder failure.

The current framework aims to quantify the $P_{hf|a}$, i.e., the probability of hull girder failure considering that collision or grounding happened. In the case of the probability of an accident ($P_{a|enc}$), as discussed in the Introduction, various tools have already been developed to quantify that. In case of consequences (C_{hf}), some tools also have been developed in our previous studies, including tankers [32,44,71]. Nevertheless, in the case of hull girder failure, which is the most tremendous structural failure, we can consider the consequences of loss of ship, cargo, and major oil outflow. Those tools could be integrated with a proposed framework in future studies to propose a holistic risk-based ship design methodology.

As shown in Fig. 1, first, multiple damage extent cases are generated using Monte Carlo simulations based on the ship's cross-section data. Second, given the ship's age, the degradation level is considered and further distributed within the structural elements composing the cross-section, accounting for variation in corrosion levels. Third, the ultimate strength of the ship hull is calculated for all cases, accounting for the damage due to collision or grounding and for corrosion degradation using an iterative approach (i.e. ultimate strength is determined by iterative increase of curvature and determination of neutral axis for considered cases of damage or grounding), taking the neutral axis rotation into account as well. This gives the probability distribution of the hull girder's ultimate strength. Fourth, this result is further used in a reliability analysis approach, accounting for additional sources of load uncertainties, in particular wave load and loading conditions. Details about the methods applied in each of these steps in the overall framework are provided in the subsections below. To facilitate computational analyses, the framework was implemented by in-house developed Python code, leveraging existing code for the structural reliability analysis, using UQ[py]lab framework [72].

2.1. Damage due to collision/grounding

In an earlier proposed approach to analyse the probability of hull girder failure [64], the damage size due to collision was taken as a single deterministic scenario, as given by the CSR [73], which takes a conservative approach. Referring to Fig. 1, the first step in the proposed framework here consists of randomly generating a large set of collision and grounding damage cases. This is achieved using the probability distributions introduced by IMO [74], which sets requirements for the damage conditions to be considered for alternative design of tanker ships.

2.1.1. Damage due to collision

According to [74], the collision-induced damage extent on a ship's cross-section is characterized using three independent random variables with given probability distribution functions: transverse penetration, vertical extent and vertical location (measured with respect to the middle of the damaged area). These functions are shown in Fig. 2.

The transverse penetration z_t is defined as the damage extent measured inwards from the ship side relative to the ship's breadth. The vertical extent z_v is considered relative to the ship's depth. Finally, the vertical location z_l is the location of the middle of the damage with respect to the ship's depth, where $z_l = 0$ corresponds to the baseline and $z_l = 1$ denotes the position of the deck.

2.1.2. Damage due to grounding

In the case of grounding, the damage extent is described similarly as for collision, relying on information from [74] as well. Thus, the damage extent is characterized using three independent random variables with given probability distribution functions: transverse extent, transverse location, and vertical penetration, as shown in Fig. 3.

The transverse extent b is defined as the damage extent relative to the ship's breadth. The vertical penetration b_v is the vertical damage extent measured from the bottom of the ship upwards, relative to the ship's depth. The transverse location b_l considers the middle position of the damage extent, relative to the ship's breadth.

2.1.3. Implementation of the damage cases in the proposed framework

In each damage scenario, three independent random variables characterize the damage extent in collision or grounding. In the proposed framework, 10,000 samples are generated as inputs for determining the corrosion degradation in the hull elements and the calculation of ultimate strength, see Fig. 1. To achieve a representative distribution of each random variable within the design space, the Latin Hypercube Sampling method is used [75]. For each sample, the respective corrosion scenario is simulated as described in detail in Section 2.2, and the ultimate strength for the hull girder in the damage case is calculated as described in Section 2.3.

2.2. Corrosion degradation modelling

Referring to Fig. 1, the second step in the proposed framework is determining the corrosion degradation level in particular elements of the damaged hull's cross-section. The adopted corrosion model to achieve this considers two effects:

- the mean thickness reduction of an element of the ship's cross-section, based on the considered degradation level;
- in the calculation of the ultimate strength of a particular element in the ship's cross-section (see Section 2.3), the calculated value of ultimate strength obtained with a mean thickness reduction is corrected using a factor which accounts for the nonuniform distribution of thickness within the element and the decrease of mechanical properties caused by corrosion.

The proposed corrosion model uses recent scientific advancements, which found that if corrosion is accounted for only as a uniform thinning of elements, the structural strength characteristics may be significantly overestimated [76]. Further, experimental and advanced numerical studies found that taking into account nonuniform thickness reduction and decrease in mechanical properties of steel, the ultimate strength can be accurately predicted [77]. However, the straightforward adoption of this complex phenomenon in an iterative approach (described in Section 2.3) for calculating the hull girder's ultimate strength is not possible since it relies on analytical formulations for the determination of stress–strain curves for particular elements composing ship's cross-section where thickness is only one variable of particular value. Thus, another approach is adopted, which consists of first calculating the ultimate strength considering only the mean thickness reduction due to corrosion, which is then multiplied by a correction factor. This *Correction Factor* (CF) is defined as follows:

$$CF = \frac{RL_{Experiment}}{RL_{Formula}} \quad (2)$$

$$RL = \frac{F_{corroded}}{F_{non-corroded}} \quad (3)$$

where: RL is the relative loss of ultimate strength accounting for the effect of corrosion, $F_{corroded}$ is the ultimate strength for the corroded element, and $F_{non-corroded}$ is the ultimate strength for the non-corroded element. Thus, $RL_{Experiment}$ is the relative loss of ultimate strength obtained experimentally [78] accounting for the exact impact of corrosion degradation, and $RL_{Formula}$ is a relative loss of ultimate strength

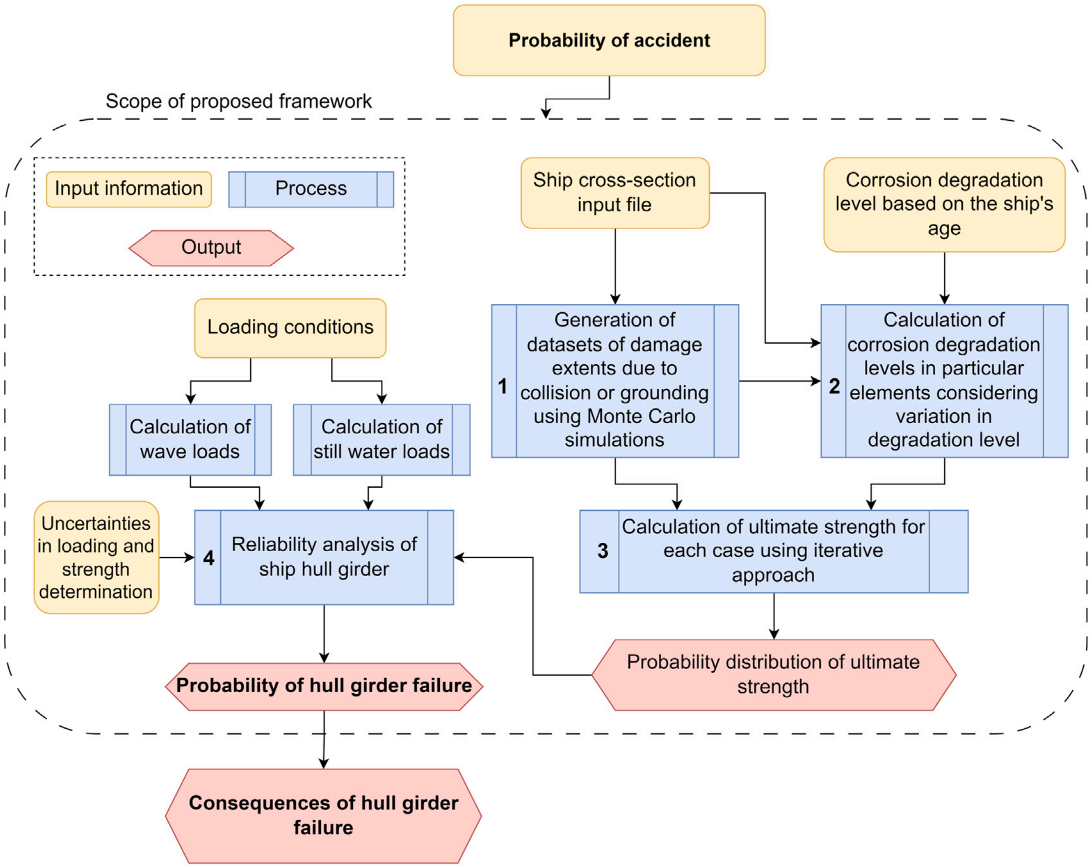

Fig. 1. Block scheme of the presented framework for hull girder failure probability assessment for accidental damage considering corrosion effects.

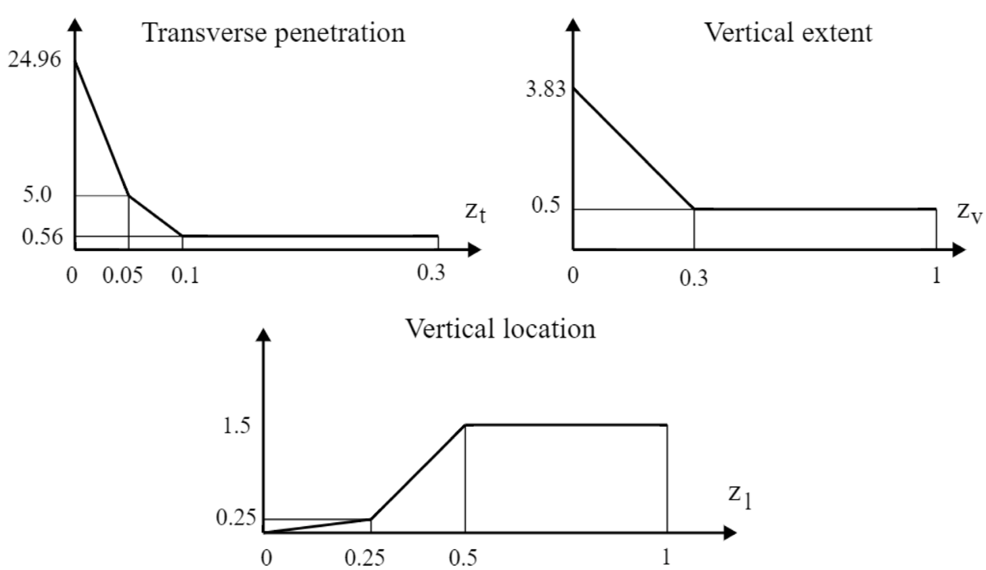

Fig. 2. Probability functions to characterize the damage extent on a ship's hull due to collision: transverse penetration, vertical extent, and vertical location.

calculated using an analytical formulation that is adopted in the iterative approach (see Section 2.3), which considers corrosion only as uniform thickness reduction. The approach employing CF to capture corrosion impact is described in detail in [52], where it was validated with experiments of corroded box girders subjected to vertical bending, showing very good accuracy.

Based further on the results presented in [52], the CF is applied in the current framework, considering the uncertainty associated with its prediction value (see Fig. 4). The CF is presented in function of the *Degree of Degradation* (DoD), which is calculated as follows:

$$DoD = \frac{A_0 - (b \cdot t_{p,corr} + A_{s,corr})}{A_0} \tag{4}$$

where b is the width of the plating, $t_{p,corr}$ is the mean thickness of the plating after corrosion, $A_{s,corr}$ is the stiffener cross-section area after corrosion, and A_0 is the initial cross-section area of the stiffened plate (without corrosion). The stiffener cross-section after corrosion $A_{s,corr}$ is determined based on the mean thickness reduction of the web and

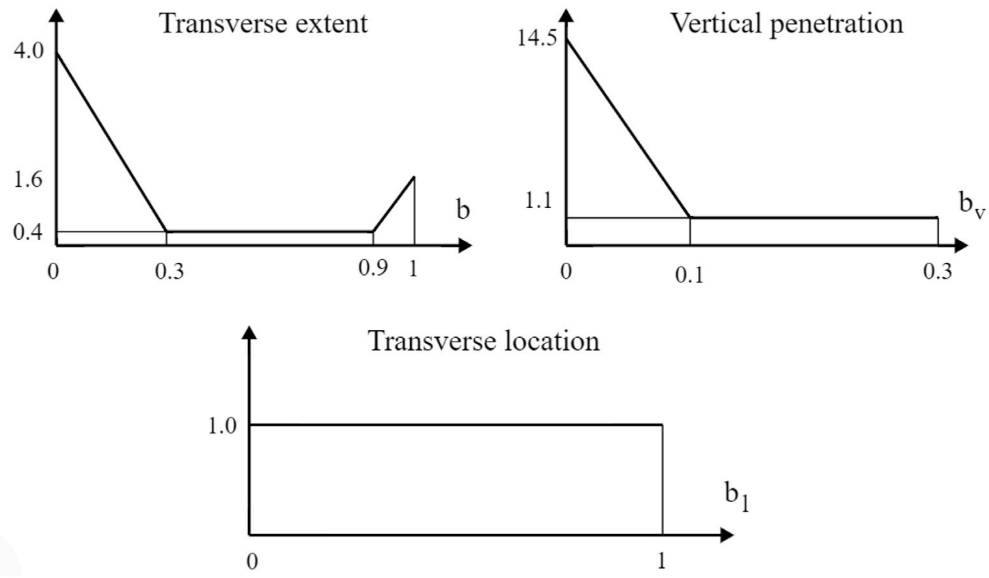

Fig. 3. Probability functions to characterize the damage extent on a ship's hull due to grounding: transverse extent, transverse location, and vertical penetration.

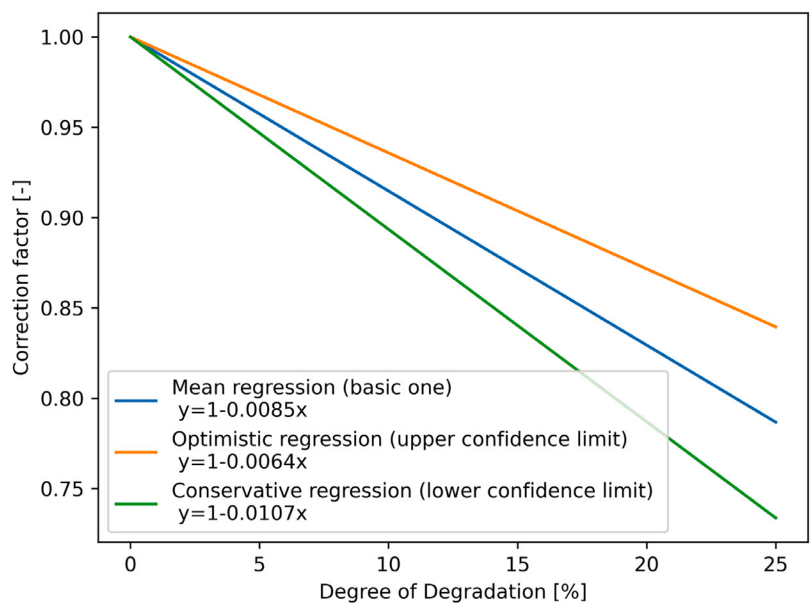

Fig. 4. Correction factor to account for the reduction in ultimate strength of a structural element considering corrosion impact in relation to the Degree of Degradation, based on [52].

flange, respectively. This is important since DoD captures the relative loss of thickness in the element, regardless of the exploitation time. Thus, although in reference work [52], the coating was not considered, it allows the use of these results in real cases when the coating is present, preventing corrosion degradation during the initial period of exploitation time. In the case of pure plate-type or hard corner elements, the factor in the equation related to the stiffener is neglected.

As shown in Fig. 4, apart from the mean value, also the upper and lower confidence levels are provided, which correspond to 2.5% and 97.5% of the cumulative probability, respectively. Based on those data, the assumption is made that the CF for a particular degradation level DoD can be represented by a normal distribution, and the moments of that distribution can be obtained. The upper confidence level corresponds to $\mu + 1.96\sigma$, whereas the lower confidence level corresponds to $\mu - 1.96\sigma$, where μ is the mean value of the distribution, and σ the standard deviation. To account for uncertainty about the CF, firstly, the DoD for each cross-section element is calculated, which varies between elements. Then, the normalized random distribution ($\mu = 0$, $\sigma = 1$) is generated for the entire cross-section, which is taken to be representative of the whole ship cross-section. To calculate the CF for a particular element, it needs to account for the mean value and standard deviation for the CF, which depends on DoD of the particular cross-section element as shown in Fig. 4. Thus, the Correction Factor for a particular element is given by the equation:

$$CF(DoD) = CF_{mean}(DoD) + Sample(N(0,1)) \cdot CF_{StDev}(DoD) \tag{5}$$

where $Sample(N(0,1))$ is a sample from the normalized distribution, where moments of this distribution (i.e. mean and standard deviation) are satisfied within the cross-section; $CF_{mean}(DoD)$ and $CF_{StDev}(DoD)$ are mean value and standard deviation of CF depending on DoD, defined as follows:

$$CF_{mean}(DoD) = 1 - 0.0085 \cdot DoD \tag{6}$$

$$CF_{StDev}(DoD) = 0.001097 \cdot DoD \tag{7}$$

The degradation level of all elements composing the cross-section must be known to calculate the CF. In an earlier deterministic approach to determine the hull girder probability [64], the method proposed in CSR [73] was adopted to model the thickness loss in cross-section elements. In this approach, the corrosion level within the cross-section is taken as a deterministic value resulting in a thickness reduction equal to half of the corrosion additions, which corresponds to a 25 year ship exploitation duration, which includes that for some time coating is active and no corrosion exists. Although this assumption is reasonable as an initial method to consider corrosion, and leads to an easily applied rule in the ship design stage, the corrosion level in actual conditions usually varies significantly within the cross-section [79]. Therefore, in the framework presented here, a probabilistic approach to account for the distribution of the corrosion degradation level across the cross-section is proposed. To this effect, corrosion additions as described in the CSR are also applied, but additional information available in Technical Background for these rules will be accounted for and implemented [80].

The corrosion additions (t_c) in the CSR were determined based on the almost 400,000 data points gathered from operating tanker ships, considering the different locations of an element within the cross-section. Thus, this approach considers different corrosion environments depending on the location of the structural member. This results in different corrosion losses depending on element position (e.g. higher corrosion diminution near the deck area) in a deterministic sense. Additional variability is introduced in the current framework through probabilistic sampling. This results in consideration of both variability in corrosion loss due to the position of an element in cross-section and uncertainty of this value due to the randomness of the corrosion process. The corrosion addition value was calculated based on the assumption that after 25 years of exploitation, the value of thickness reduction in a single element (plate or stiffener) will be lower than the associated corrosion addition with a probability equal to 90%. In other words, the local thickness reduction may possibly exceed the corrosion addition value in 10% of cases. Furthermore, according to information in the above-referenced CSR Technical Background, the thickness reduction itself follows a log-normal probability distribution (see Fig. 5). It was found that for the ultimate strength calculation, which considers the entire ship hull cross-section and not a single element, a degradation level equal to 50% of corrosion addition values could be taken as thickness reduction achieved within the whole cross-section. This corresponds to approx. mean thickness reduction within the entire hull girder cross-section after 25 years of exploitation. This deterministic approach is rational for rule requirements. However, by considering the distribution of degradation level within the hull cross-section as the percentage of corrosion addition, we can normalize the distribution, regardless of the absolute value of particular corrosion addition. Thus, it is justified to take $0.5t_c$ as the mean value and t_c as the 90th percentile value of the log-normal distribution. Having these two values, the moments of the log-normal distribution (mean value and standard deviation) can be calculated easily, resulting in a mean value of 0.5 and a standard deviation of 0.328. Those moments define the log-normal distribution of degradation level considered as a percentage of absolute values of corrosion additions in particular cross-section elements. Then, by sampling this lognormal distribution using the Monte Carlo method and multiplying this by corrosion additions in particular elements, a more realistic thickness spread is obtained, considering that the moments of the normalized distribution correspond to those of experimentally determined values, within the cross-section. The thickness reduction t_{red} for a particular element can thus be written as:

$$t_{red} = t_c \cdot Sample(Lognormal(0.5, 0.328)) \tag{8}$$

2.3. Calculation of ultimate strength

Referring to Fig. 1, the third step in the proposed framework is the calculation of the ultimate strength of the hull girder. To achieve this, the so-called “iterative” approach is used. This method was initially developed by Smith [81] and further implemented in the Common Structural Rules (CSR) for Tankers and Bulk Carriers [73]. In this method, the ship's cross-section is first divided into different types of elements (plates, stiffened plates and hard corners). Then, the ultimate strength of each individual element is calculated using appropriate physics-based formulations (see [73]), resulting in a stress–strain relationship for each element. Subsequently, the ultimate strength of the entire cross-section is calculated iteratively, where in each iteration, the bending curvature is incrementally increased. Based on this ultimate strength analysis, the strains and the corresponding stresses in each element are calculated. Finally, the position of the neutral axis is determined, based on the requirement that the sum of all forces in the elements should equal zero.

A drawback of the classical method is that it considers a symmetrical cross-section, i.e. it does not account for the rotation of the neutral axis. However, in damaged conditions, the cross-section would no longer be symmetrical, necessitating consideration of the rotation of the neutral axis. In the present framework, this is accounted for using an approach suggested by [65], in which the following equation for pure vertical bending is solved iteratively :

$$\begin{Bmatrix} 0 \\ \Delta M_V \end{Bmatrix} = \begin{bmatrix} D_{HH} & D_{HV} \\ D_{VH} & D_{VV} \end{bmatrix} \begin{Bmatrix} \Delta\phi_H \\ \Delta\phi_V^0 \end{Bmatrix} \tag{9}$$

where ΔM_V is the increment of the vertical bending moment, D_{HH}, D_{VV}, D_{HV}, D_{VH} are the flexural stiffnesses of the cross-section calculated according to the actual centroid and respective axes (horizontal, vertical), $\Delta\phi_H$ is the increment of the horizontal curvature, and $\Delta\phi_V^0$ is the increment of the vertical curvature (which is considered as constant value).

Considering a constant vertical curvature increment ($\Delta\phi_V^0$), the Eq. (9) yields the following results [65]:

$$\Delta\phi_H = -\frac{D_{HV}}{D_{HH}}\Delta\phi_V^0 \tag{10}$$

$$\Delta M_V = \left(D_{VV} - \frac{D_{VH} D_{HV}}{D_{HH}} \right) \Delta\phi_V^0 \tag{11}$$

The hull girder's ultimate strength is calculated as the peak value from the $M_V - \phi_V$ curve.

The iterative method, as implemented in the current framework, was already validated with experiments of corroded box girders subjected to pure vertical bending in [52], showing very good accuracy and need for consideration of the Correction Factor. An additional analysis was performed to show the applicability of this approach to situations of severely damaged cross-sections and to check if the method was properly implemented. Very recently, experimental results of two steel box girders subjected to vertical bending were presented in [82], having simulated damage due to collision as a hole and more details about exact structural dimensions and material properties can be found herein.

The comparison between the results obtained using an iterative approach implemented in on-house software and the experiment [82] is presented in Fig. 6, considering moment–curvature relationships. It could be noted that there are no significant discrepancies between the computations and experiments, considering both quantitative and qualitative assessments. Very good convergence was obtained, especially for inclined conditions, where the moment–curvature curve and ultimate capacity are very similar. The ultimate capacity, in this case, is equal to 609 kN m for the iterative method and 580 kN m for the experiment. A more prominent difference is observed for the model in an upright condition. In this case, the ultimate capacities are equal to 680 kN m and 609 kN m, for computational approach and experiment, respectively.

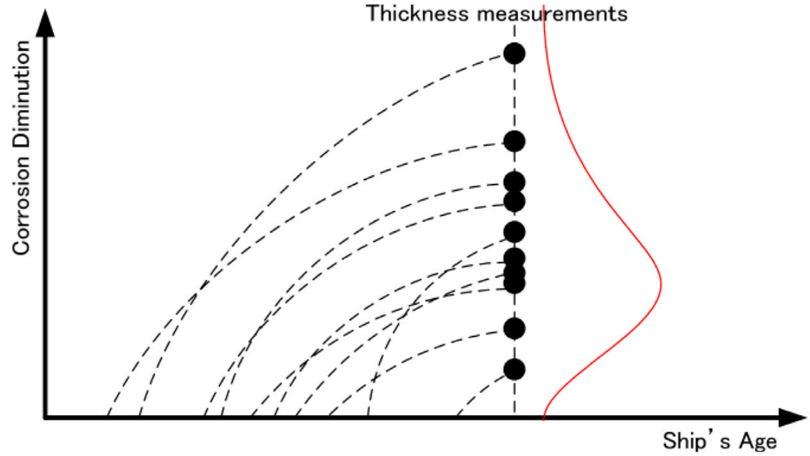

Fig. 5. Corrosion diminution within the ship hull cross-section after 25 years of exploitation based on measurements modelled as log-normal distribution [80].

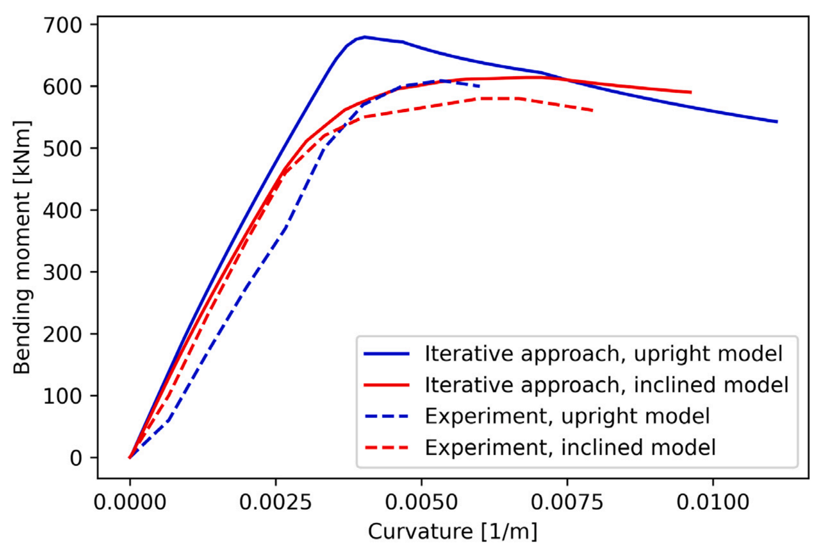

Fig. 6. Comparison between iterative approach implemented in our framework with experimental results of damaged sections presented in [82].

In both cases, the computations slightly overestimated the ultimate strength value. This bias could be due to some uncertainties typical for such experiments, i.e. adopted boundary conditions, variation in mechanical properties, initial plating imperfections, etc. Secondly, the experiment considered two samples only, so we cannot draw more general conclusions of a statistical nature. Nevertheless, the presented results show that the iterative approach is a very good method for ultimate strength evaluation, especially since more advanced computational methods (such as FEM) are, in many cases, subjected to bigger uncertainty and very sensitive to adopted modelling assumptions, as was demonstrated in recent ISSC benchmark study [83]. To account for the epistemic uncertainty of the adopted method, the uncertainty factor $\widetilde{x_U}$ is considered as described in Section 2.4.

2.4. Reliability analysis

Referring to Fig. 1, the fourth step in the proposed framework is the calculation of the probability of hull girder failure. To achieve this, the reliability analysis approach is applied, similarly as presented by [62] for a similar problem. In the current study, the Monte Carlo sampling method [84] is used to determine the probability of failure. In the deterministic approach, very rare events are taken as design scenarios, leading to a conservative approach to assessing ship design risk. Such conservatism has been argued against in risk analysis [85], suggesting that a more comprehensive consideration of uncertain quantities is preferable. The reliability analysis allows for such a quantitative analysis of the failure probability. In this view, multiple probable damage scenarios are accounted for, requiring the designer and/or regulator to explicitly consider what probability of failure is acceptable, leading to a more rational design [1].

In the reliability analysis, the limit state function g is defined as follows:

$$g = \widetilde{x_U}\,\widetilde{M_U} - \widetilde{x_{SW}}\,\widetilde{M_{SW}} - \widetilde{x_W}\,\widetilde{x_S}\,\widetilde{M_{WV}} \tag{12}$$

where $\widetilde{M_{SW}}, \widetilde{M_{WV}}, \widetilde{M_U}$ are the still water bending moment, the wave bending moment, and the ultimate strength capacity of the damaged hull girder subject to corrosion degradation, which are all considered as random variables. The variables $\widetilde{x_U}$, $\widetilde{x_{SW}}$, $\widetilde{x_W}$ and $\widetilde{x_S}$ express further modelling uncertainties as a probabilistic adjustment factor formulation, as conceptually explained in [86]. These are described below.

The ultimate strength $\widetilde{M_U}$ is based on the computations as described in Sections 2.1–2.3 (see Fig. 1). The probability distribution is obtained by Monte Carlo simulations, considering uncertainties associated with the accidental damage and the effects of corrosion degradation. Thus, this variable $\widetilde{M_U}$ covers the aleatory uncertainty related to the input variables. However, the epistemic uncertainty related to the adopted computation method itself, i.e. the model uncertainty, is not considered in this expression. This model uncertainty is therefore accounted for through the variable $\widetilde{x_U}$, which accounts for the assumptions considered in the modelling, inadequacy of engineering models, simplifications, etc. Recently, a robust quantification of uncertainty of the iterative approach for determination of ultimate strength was presented in [87], where it was concluded that it could be modelled via a normal distribution. Thus, in the current framework, the model uncertainty associated with the ultimate strength capacity calculation for double-hull oil tankers is accounted for as follows:

$$\widetilde{x_U} \sim N\{1, 0.08\} \tag{13}$$

for sagging, and:

$$\widetilde{x_U} \sim N\{1, 0.04\} \tag{14}$$

for the hogging case.

Similarly, $\widetilde{x_{SW}}$ is a probabilistic adjustment factor variable accounting for the model uncertainty concerning the still water bending moment prediction; $\widetilde{x_W}$ accounts for the model uncertainty of wave-induced bending moment predictions due to the use of a linear method, whereas $\widetilde{x_S}$ takes into account nonlinearities in the determination of loads in the sagging condition. In the case of hogging, the nonlinearities do not need to be taken into account for wave loads determination [88]. The values for these probabilistic variables are determined from previous studies [88,89] and follow normal distributions:

$$\widetilde{x_{SW}} \sim N\{1, 0.1\} \tag{15}$$

$$\widetilde{x_W} \sim N\{1, 0.1\} \tag{16}$$

$$\widetilde{x_S} \sim N\{1, 0.1\} \tag{17}$$

Finally, the random variables determining still-water and wave-induced loads need to be determined. In the case of the still water bending moment, it needs to be considered that this moment can significantly increase due to flooding of the damaged compartments [61,70]. This previous research has indicated that still water loads in damaged conditions can reach a level of 2.5 times that of the water loads in intact conditions. Therefore, this effect should be considered in reliability analyses of damaged ship hulls. In the current framework, the results of the analysis presented in [69] are applied, where the probability distribution of the still water bending moment was calculated for tanker ships accounting for the same damage distributions [74] as considered in the current study, see Section 2.1. The probability distribution of still water loads in damage conditions is given by the following equation:

$$\widetilde{M_{SW}} = M_{SW-design}\widetilde{K_{SW}} \tag{18}$$

where $M_{SW-design}$ is the deterministic value of the design still water bending moment and $\widetilde{K_{SW}}$ is the random variable considered as a multiplication factor. This factor is given by a normal distribution:

$$\widetilde{K_{SW}} \sim N\{0.72, 0.56\} \tag{19}$$

for damage due to collision, and:

$$\widetilde{K_{SW}} \sim N\{0.56, 0.88\} \tag{20}$$

for damage due to grounding.

In the case of intact conditions, K_{SW} equals 1.0 as a deterministic value without distribution. Since water loads are determined by the hydrostatic calculations as given in the loading manual, they are not subject to high uncertainty levels. In this case, the uncertainty of the determination of still water loads is considered by a factor $\widetilde{x_{SW}}$, as given in the limit state function (Eq. (12)). In the case of damaged conditions, the mean value of K_{SW} is lower than one, indicating that due to flooding, in many cases, still water loads are lower than in intact conditions. However, one needs to note that there is a very high standard deviation. This leads to significantly increased still water bending moment in approx. 40% of cases, reaching the maximum level of $K_{SW} = 1.9$ in case of collisions and $K_{SW} = 2.7$ for grounding. Those extreme cases are very important in view of reliability analysis.

Finally, the question is if this factor should be considered the same in hogging (associated with ballast condition) and sagging (associated with full load condition). The CSR considers the multiplication factor of still water bending moment in damaged conditions equal to 1.1 regardless of the loading type [73], which seems to be too optimistic from a risk-based perspective, given the previous discussion. On the other hand, the values of K_{SW} equal to 1.1 and 1.5 were proposed in [90] for hogging and sagging, respectively. Other works focused mainly on determination of this factor in sagging [61,70,91], with values reaching level of 2.4. Since there is no consensus about the discussed issue, in the current study, the aforementioned values of K_{SW} distribution are considered the same for both full-load and ballast conditions. This is considered rational from a risk-based perspective, allowing the drawing of a more conservative assessment of failure probability.

In the case of the wave loads, the deterministic values given in the CSR [73] are modelled by a Weibull distribution with a probability of exceedance of 10^{-8}. Based on that, the distribution of extreme values of wave-induced bending moment over a specified time period can be modelled as a Gumbel distribution with the following parameters [92]:

$$\mu = q(ln(n))^h \tag{21}$$

$$\beta = \frac{q}{h}(ln(n))^{\frac{1-h}{h}} \tag{22}$$

where μ and β are the parameters of the Gumbel distribution, n represents the number of load cycles over the reference time period T_r for a given mean period value of the wave T_w. Relying on information in the above reference, it is considered that $T_r = 1$ yr, and $T_w = 8$ s. The q and h are parameters of the Weibull distribution and can be determined depending on the ship length and rule wave bending moment as given in the same Ref. [92].

As found in the HARDER project, only approx. 11% of collisions happen in open seas, whereas 89% occur in the harbour and coastal waters with significantly milder wave conditions [91]. Similar observations were reported very recently in [93] where only 651 of 8923 maritime accidents (of various types) took place in open sea areas based on 40-years statistics of Norwegian coastal waters. In the case of grounding, we can consider that 100% of accidents happen in the harbour and coastal waters since a low draught is needed for grounding to occur. This is supported by the data, where the maximum distance from the shore of grounding accidents based on historical data was found to be equal to approx. 10 nm for North America [94] and similar observations were made for the Gulf of Finland [24]. Thus, the parameters of Weibull distribution (q and h) should be determined separately for open seas and coastal/harbour waters. The coastal/harbour waters could be associated with the harbour/sheltered water design load scenario as defined in CSR [73]. Thus, the rule wave bending moment can be calculated considering the reduced value by 60% compared to the unrestricted area of service, as given in the Rules [73]. This will result in milder wave conditions in that area.

Thus, the probability of failure will be considered for collision accident as the sum of conditional probabilities, equal to:

$$P_{coll} = 0.89P_{harbour} + 0.11P_{open} \tag{23}$$

where $P_{harbour}$ is the probability of failure in coastal/harbour waters, and P_{open} is the probability of failure in open seas. In the case of grounding, the probability of failure is associated with $P_{harbour}$.

Notably, both the still water loads and wave loads are dependent on the loading condition. It is taken that 40% of the vessel's lifetime, it operates at a full-loading condition, with 40% of the time in ballast condition, 10% of the time in a partial loading condition, with the

Table 1
Summary of still water and wave loading parameters of probability distributions — VLCC tanker ship.

Accident type	Loading condition	$\widetilde{M_{SW}}$ [kN m]		$\widetilde{M_{WV}}$ [kN m]			
		Mean	St. Dev.	Coastal/harbour		Non-restricted area	
				μ	β	μ	β
No accident (Intact)	Full load	6 158 576	–	–	–	5 403 182	685 991
	Ballast	7 551 120	–	–	–	5 403 182	685 991
Grounding	Full load	3 448 803	5 419 547	2 136 368	277 133	–	–
	Ballast	4 228 627	6 644 986	2 136 368	277 133	–	–
Collision	Full load	4 434 175	3 448 803	2 136 368	277 133	5 403 182	685 991
	Ballast	5 436 806	4 228 627	2 136 368	277 133	5 403 182	685 991

Table 2
Summary of still water and wave loading parameters of probability distributions — handysize tanker ship.

Accident type	Loading condition	$\widetilde{M_{SW}}$ [kN m]		$\widetilde{M_{WV}}$ [kN m]			
		Mean	St. Dev.	Coastal/harbour		Non-restricted area	
				μ	β	μ	β
No accident (Intact)	Full load	301 336	–	–	–	383 882	26 900
	Ballast	347 915	–	–	–	383 882	26 900
Grounding	Full load	168 748	265 176	153 553	10 760	–	–
	Ballast	194 832	306 165	153 553	10 760	–	–
Collision	Full load	216 962	168 748	153 553	10 760	383 882	26 900
	Ballast	250 499	194 832	153 553	10 760	383 882	26 900

remaining 10% is considered a port condition [95]. In the current framework, two loading conditions are considered, i.e. full loading condition and ballast condition, since in the first one, the still water sagging bending moment is maximized and in the second, the hogging still water bending moment. As shown in earlier work [64], partial loading and port conditions have almost no impact on the final reliability index. Thus, the resulting probability of failure (P_f) is taken as the sum of probabilities of failure for full-load ($P_{f,\ full\ load}$) and ballast conditions ($P_{f,\ ballast}$), respectively, multiplied by the conditional probability of each loading scenario, as explained above:

$$P_f = 0.4P_{f,\ full\ load} + 0.4P_{f,\ ballast} \tag{24}$$

The summary of still water and wave loading parameters of distributions for reliability analysis is given in Table 1 for VLCC tanker, depending on the accident type and loading condition.

The summary of still water and wave loading parameters of probability distributions for reliability analysis is given in Table 2 for the handysize tanker, depending on the accident type and loading condition.

It needs to be noted that in the limit state function as presented in Eq. (12), both still water and wave loads have the same sign. However, considering the full load condition, the still water bending moment is negative (in sagging). In the case of ballast condition, the still bending moment is positive (in hogging). Thus, it is reflected in the limit state function. If sagging is considered, the still water bending moment in a full load scenario is superimposed with the sagging wave bending moment. If hogging is considered, the still water bending moment in ballast condition is superimposed with the hogging wave bending moment. In the rest cases (hogging in full load condition and sagging in ballast condition), the still water and wave bending moments are of opposite signs.

2.5. Description of the tanker design cases

In the present study, the framework is applied to two case studies of different tanker ships, aiming to show the applicability of the framework and to obtain initial insights on the impact of ship size. Tanker vessels are taken as case study examples since these are commonly considered as safety–critical ships, where in case of damage, catastrophic consequences leading to ecological disaster may occur (see e.g. Prestige catastrophe [96]). The tanker ships considered in the study are VLCC and handysize tankers, with their main dimensions and characteristics presented in Table 3.

Table 3
Main dimensions and key characteristics of the tanker vessels considered in the case studies.

Dimension	Symbol	VLCC	Handysize	Unit
Length over all	L	320	138	m
Moulded breadth	B	58	22.5	m
Moulded depth	D	31	12.8	m
Scantling draught	T	22	8.7	m
Block coefficient	Cb	0.83	0.78	–
Designed speed	v	16.7	14.0	kn

In the case of the VLCC tanker, the cross-section is made partially of normal-strength steel with a yield stress equal to 235 MPa and partially of higher-strength steel with a yield stress of 315 MPa. The design thickness of plating varies from 14 to 23 mm. The cross-section stiffeners are dominated by pre-fabricated T-stiffeners with a web of maximum of 600 mm height and a flange up to 220 mm width. The stiffeners' thicknesses are between 10 and 20 mm. The generic cross-section, as applied in the proposed framework, shows the division into particular cross-section elements, which is illustrated as an output from developed software in Fig. 7. Since the cross-section is symmetrical, one side of the ship is presented in Fig. 7.

The detailed cross-section data of the VLCC tanker regarding dimensions of structural elements is provided in Table 4. The numbers of elements refer to the one presented in Fig. 7.

The plating design thicknesses for the Handysize tanker are between 9 and 14 mm. The majority of stiffeners are bulb profiles ranging from 180 × 10 up to 300 × 11 types, and some minor stiffeners are flat profiles with size 100 × 10. The entire cross-section is made of normal-strength steel with yield stress equal to 235 MPa. The generic cross-section, as applied in the proposed framework, shows the division into particular cross-section elements, which is illustrated as an output from developed software in Fig. 8. Since the cross-section is symmetrical, one side of the ship is presented in Fig. 7.

The detailed cross-section data of the Handysize tanker regarding dimensions of structural elements is provided in Table 5. The numbers of elements refer to the one presented in Fig. 8.

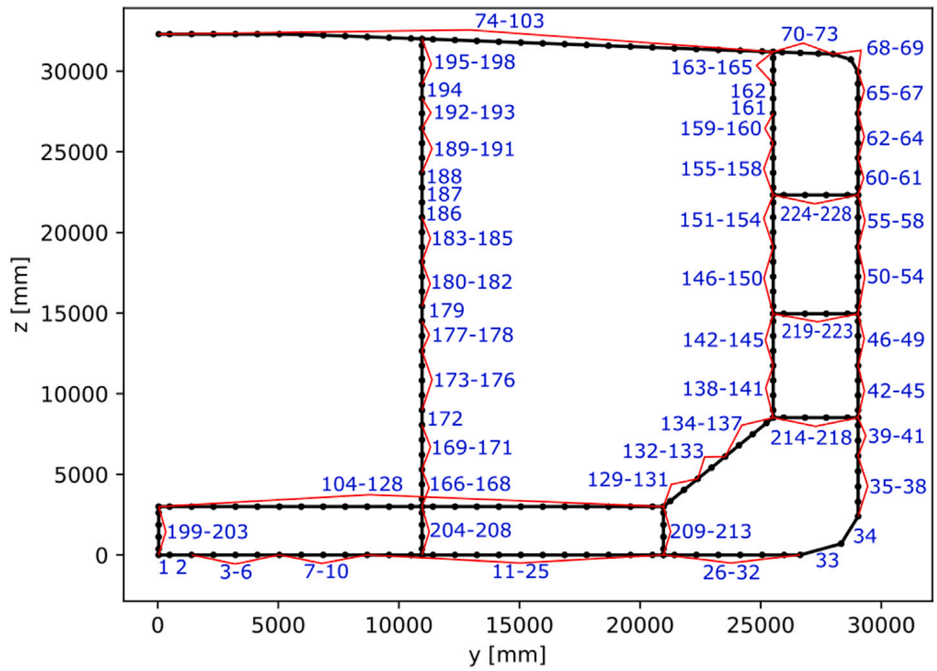

Fig. 7. Cross-section of VLCC tanker ship applied in the case study.

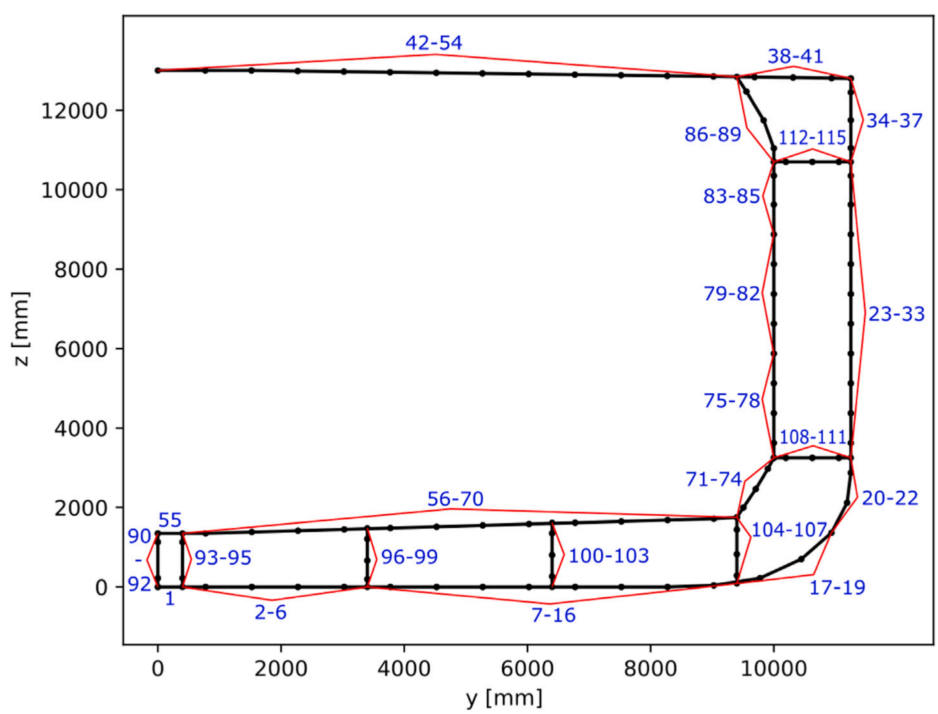

Fig. 8. Cross-section of Handysize tanker ship applied in the case study.

3. Results

In this Section, various results of analyses performed to show the applicability of the framework are presented. First, considering the case study of the VLCC tanker ship, two types of sensitivity analyses are performed to show the impact of modelling approaches adopted in the here proposed framework. The first sensitivity analysis, presented in Section 3.1, compares the deterministic and probabilistic modelling approaches of damage size, and the associated impacts on the resulting ultimate strength. In this analysis, corrosion degradation is modelled deterministically. The second sensitivity analysis, presented in Section 3.2, compares different approaches to model corrosion degradation

Table 4
Cross-section data of VLCC tanker ship.

Element numbers	Structural element	Shell thickness [mm]	Stiffener spacing [mm]	Stiffener dimensions	Steel type
1–2	Bottom shell	23	910	T 580 × 12 + 200 × 20	AH32
3–6		22	910	T 580 × 12 + 200 × 20	AH32
7–10		21	910	T 580 × 12 + 200 × 20	AH32
11–25		20	910	T 580 × 12 + 200 × 20	AH32
26–32		20	910	T 620 × 12 + 200 × 20	AH32
33–34	Bilge	20	–	–	AH32
35–38	Outer shell	20	950	T 620 × 12 + 200 × 20	AH32
39–41		22	950	T 670 × 13 + 220 × 20	A
42–45		20.5	920	T 630 × 12 + 180 × 20	A
46–49		20.5	920	T 580 × 12 + 180 × 20	A
50–54		20.5	920	T 520 × 12 + 170 × 20	A
55–58		20.5	920	T 500 × 12 + 150 × 18	A
59–61		20.5	920	T 420 × 12 + 130 × 18	A
62–64		20.5	920	T 390 × 12 + 130 × 15	A
65–67		19	920	L 350 × 150 × 12/17	AH32
68–69	Sheer strake	19	–	–	DH32
70–73	Upper deck	21	750	FB 330 × 20	AH32
74–103		21	910	T 630 × 12 + 200 × 20	AH32
104–128	Inner bottom	19.5	910	T 630 × 12 + 200 × 20	AH32
129–131	Hopper tank top	19	895	T 600 × 12 + 200 × 20	AH32
132–133		19	895	T 580 × 12 + 200 × 20	AH32
134–137		19	895	T 580 × 12 + 180 × 20	AH32
138–141	Side longitudinal bulkhead	20	920	T 620 × 12 + 180 × 20	A
142–145		19	920	T 570 × 12 + 180 × 20	A
146–150		17	920	T 510 × 12 + 180 × 20	A
151–154		16	920	T 500 × 12 + 150 × 18	A
155–158		15	920	T 430 × 12 + 130 × 18	A
159–160		15	920	T 400 × 12 + 130 × 15	A
161		20	920	L 350 × 100 × 12/17	AH32
162		20	920	T 1020 × 12 + 150 × 16	AH32
163–165		20	755	L 350 × 100 × 12/17	AH32
166–168	Longitudinal bulkhead	19.5	920	T 610 × 12 + 200 × 20	AH32
169–171		21	920	T 580 × 12 + 200 × 20	AH32
172		21	920	T 1500 × 12 + 180 × 20	A
173–176		19.5	920	T 630 × 12 + 200 × 20	A
177–178		19.5	920	T 600 × 12 + 180 × 20	A
179		18	920	T 1400 × 12 + 180 × 20	A
180–182		18	920	T 550 × 12 + 180 × 20	A
183–185		17	920	T 500 × 12 + 160 × 20	A
186		16.5	920	T 480 × 12 + 150 × 18	A
187		16.5	920	T 1020 × 12 + 150 × 16	A
188		16.5	920	T 480 × 12 + 150 × 18	A
189–191		16.5	920	T 430 × 12 + 150 × 15	A
192–193		16.5	920	T 400 × 12 + 150 × 15	A
194		18	865	T 1020 × 12 + 150 × 16	AH32
195–198		18	810	L 350 × 100 × 12/17	AH32
199–203	Double Bottom girders	17	750	L 350 × 100 × 12/17	AH32
204–213		15	750	FB 150 × 13	AH32
214–223	Lower decks	15	880	L 150 × 90 × 12	A
224–228		14	880	L 150 × 90 × 12	A

in view of thickness and strength loss, and the associated impact on the resulting ultimate strength. In this analysis, the undamaged cross-section of the VLCC tanker is applied. Finally, the overall reliability analyses are performed for both tanker design case studies, showing the applicability of the proposed framework, see Section 3.3.

3.1. *Sensitivity analysis: Influence of considered damage model on ultimate strength*

In this section, two approaches are compared to analyse how accidental damage influences the ultimate strength: a deterministic and probabilistic approach. The former deterministic approach is the one taken in the CSR to estimate the residual strength at the design stage [73]. In this approach, a rather conservative deterministic damage size is applied to the ship hull due to either collision or grounding, as shown in Fig. 9. The collision-induced damage has dimensions breadth $d = B/16$ and height $h = 0.6D$, where B is the ship breadth and D is the ship depth, respectively. The grounding-induced damage has dimensions breadth $b = 0.6B$ and height $h = min(B/15, 2\text{ m})$.

In the probabilistic approach, outlined in Section 2, to compare the influence of the accidental damage models, only a deterministic thickness loss due to corrosion is applied (implemented as a reduction equal to half of the corrosion additions), without further considering the CF described in Section 2.2. Thanks to that, we can capture the impact of damage modelling type on the resulting ultimate strength without disturbances brought by the uncertainties due to corrosion degradation. This is why the deterministic corrosion model is considered for the purpose of this analysis.

An example of the Moment-Curvature relationships for collision-induced damage in the sagging condition of the VLCC tanker case is presented in Fig. 10. This shows the bending moment calculated in 10,000 simulation runs, with damage sizes sampled, as explained in

Table 5
Cross-section data of Handysize tanker ship.

Element numbers	Structural element	Shell thickness [mm]	Stiffener spacing [mm]	Stiffener dimensions	Steel type
1	Bottom shell	14	–	–	A
2–6		12	750	HP 280 × 11	A
7–16		11.5	750	HP 280 × 11	A
17–19	Bilge	11.5	870	HP 260 × 10	A
20–22		11.5	750	HP 260 × 10	A
23–33	Outer shell	11.5	750	HP 260 × 10	A
34–37		13	700	HP 180 × 10	A
39–41	Upper deck	13	625	HP 180 × 10	A
42–54		11	750	HP 220 × 10	A
55	Inner bottom	12	–	–	A
56–70		12	750	HP 300 × 11	A
71–74	Hopper tank top	11	505	HP 260 × 10	A
75–78	Side longitudinal bulkhead	11	750	HP 280 × 11	A
79–82		10	750	HP 280 × 11	A
83–85		9	750	HP 280 × 11	A
86–89		10	720	HP 260 × 10	A
90–92	Double bottom girders	14	–	–	A
93–95		12	–	–	A
96–103		9	545	FB 100 × 10	A
104–107		9	620	FB 100 × 10	A
108–115	Lower decks	10	420	HP 140 × 9	A

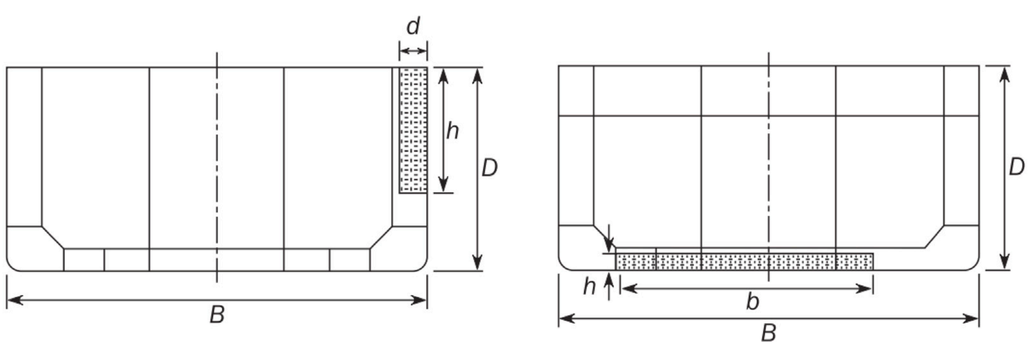

Fig. 9. Accidental damage extent due to collision (left) and grounding (right) [73].

Section 2.1. Quite a significant spread is observed in the results due to uncertainty in the determination of collision-induced damage. The peak value (in this case, minimum in sagging condition) of each curve is considered as the hull girder's ultimate strength capacity.

In Fig. 11, the histogram and probability distribution (estimated using Kernel Density Estimation (KDE) [97]) of ultimate strength is presented for the same case (collision-induced damage, sagging condition, VLCC tanker case). The bars represent the histogram, whereas the darker blue line represents the PDF estimated using KDE (a similar approach is considered for further Figs. 12–14). It is seen that the histogram does not follow any known probability distribution, with three local maxima observed. The majority of cases yield an ultimate strength capacity close to the one for a non-damaged cross-section, which indicates that in most cases, the collision-induced damage is not so severe. In addition to the histogram resulting from the probabilistic analysis, the ultimate capacity value obtained via the deterministic approach is presented as well in the figure. Overall, in the presented case, only a few simulated samples (3.3% of the total number)lead to a lower ultimate strength capacity value, showing that the deterministic approach given in the CSR is rather conservative.

The histogram of ultimate strength capacity for the grounding-induced damage in the sagging condition for the VLCC tanker case is presented in Fig. 12. Similarly to the collision case, the majority of the simulation results are concentrated around the ultimate strength capacity for a non-damaged hull, indicating that many simulated grounding damages are not very extensive. However, compared to the collision case, many more samples (16% of the total number) result in a lower ultimate strength capacity compared to the deterministically obtained value. Therefore, the CSR approach is not as conservative as in the case of collision damage. In addition, the difference between the maximum and minimum values of ultimate strength capacity is significantly higher in case of damage due to grounding, indicating that grounding accidents could be a more dangerous scenario. However, the minimum ultimate strength capacity is obtained for extremely rare events.

The histograms for the ultimate capacity for collision- and grounding-induced damage in the hogging conditions for the VLCC tanker case are presented in Figs. 13 and 14, respectively. Overall, similar trends can be observed as in the sagging case: most simulation results are concentrated around the ultimate strength capacity value associated with that of a non-damaged cross-section. This concentration is, however, higher in the collision accident case than for groundings, where a larger spread in ultimate strength capacity is observed. Similar as for the sagging condition, the deterministic value corresponds to extremely rare situations for collision, indicating that the CSR take a very conservative approach to collision damage. For the grounding case, a larger share of accident scenarios leads to a lower ultimate strength than the accident scenario in the deterministic approach, indicating a less conservative approach.

A summary of the results obtained via the two approaches to account for the accidental damage is given in Table 6, where the

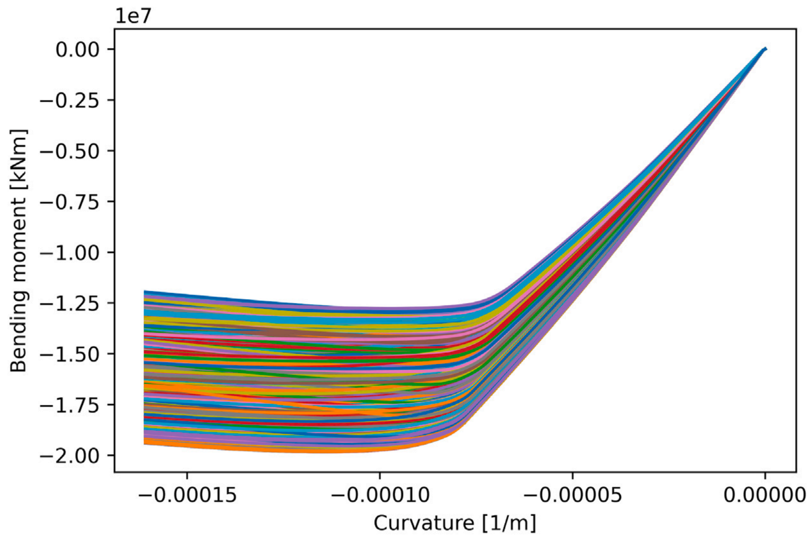

Fig. 10. Moment-Curvature relationships for probabilistic simulations considering collision-induced damage, sagging condition, VLCC tanker case.

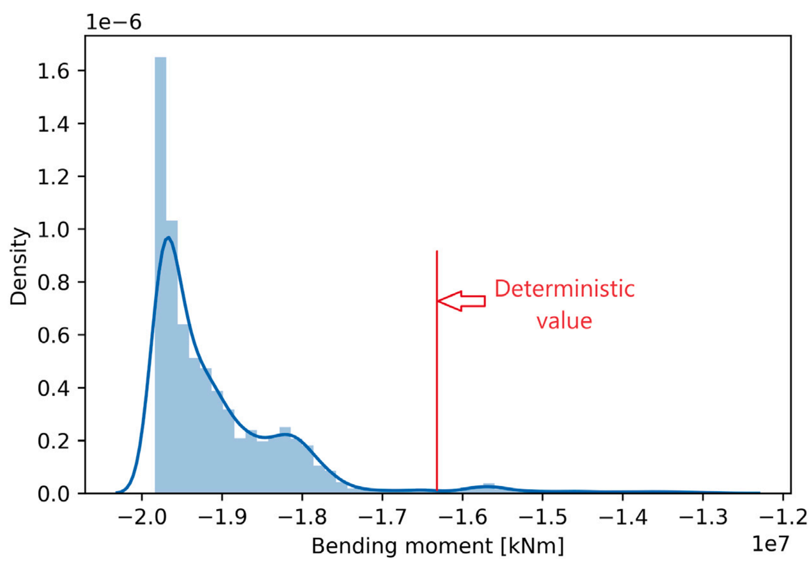

Fig. 11. Comparison of ultimate strength capacity: deterministic and probabilistic approach, collision-induced damage, sagging condition, VLCC tanker case.

Table 6
Summary of ultimate strength capacity calculations for the deterministic and probabilistic approaches to account for accidental damage, VLCC tanker case.

Dam. type	Loading	CSR [MN m]	Percentile value	Prob. Mean [MN m]	Prob. St. Dev. [MN m]	Prob. Min [MN m]
Collision	Sagging	16 362	96.7%	19 012	997	12 775
	Hogging	22 217	96.7%	24 721	944	17 900
Grounding	Sagging	17 870	84.6%	18 879	1306	8986
	Hogging	21 063	84.0%	23 287	2539	8015

Dam. type — damage type; CSR — Value from the deterministic approach as given in CSR; Prob. Mean — Mean value from probabilistic approach; Prob. St. Dev. — Standard Deviation from probabilistic approach; Prob. Min — Minimum value from probabilistic approach.

ultimate strength capacities are given as absolute values. In the case of the deterministic approach (denoted as CSR in the table), the obtained values are generally lower than the mean values obtained using the probabilistic approach. However, significant differences between the collision and grounding damage types are observed as follows:

- In case of collision, the deterministically obtained value corresponds to the 96.7 percentile value of the probabilistic distribution. This is very close to the engineering approach, which usually considers the 97.5 percentile value (which corresponds to the mean plus approx. two standard deviations of the distribution) as a conservative assumption [98].
- In the case of grounding, the deterministic value corresponds to approximately the 84 percentile value of the probabilistic distribution and the standard deviation is much higher than in the case of collision. The latter is important in view of the reliability analysis, which heavily depends on the distribution shape.
- The minimum values are much lower in case of grounding damage than for collisions, which suggests that grounding scenarios can be far more dangerous than collision scenarios, even though the mean values of capacity are rather close to each other. This

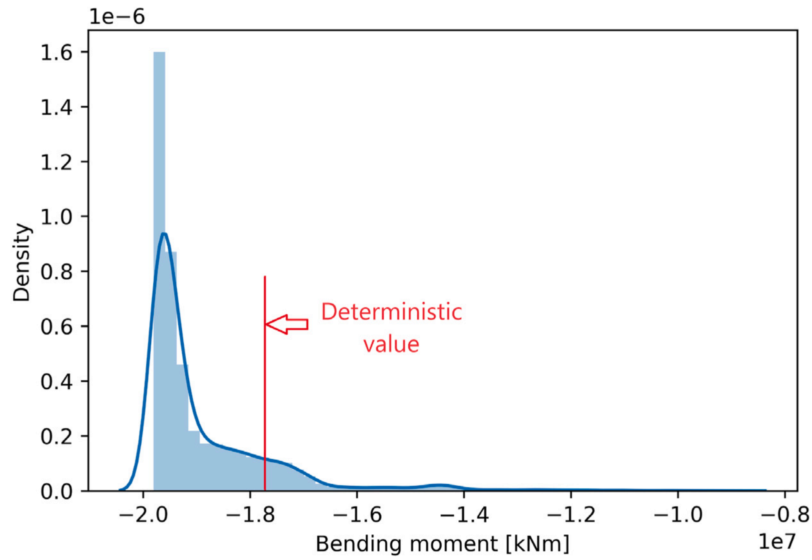

Fig. 12. Comparison of ultimate strength capacity: deterministic and probabilistic approach, grounding-induced damage, sagging condition, VLCC tanker case.

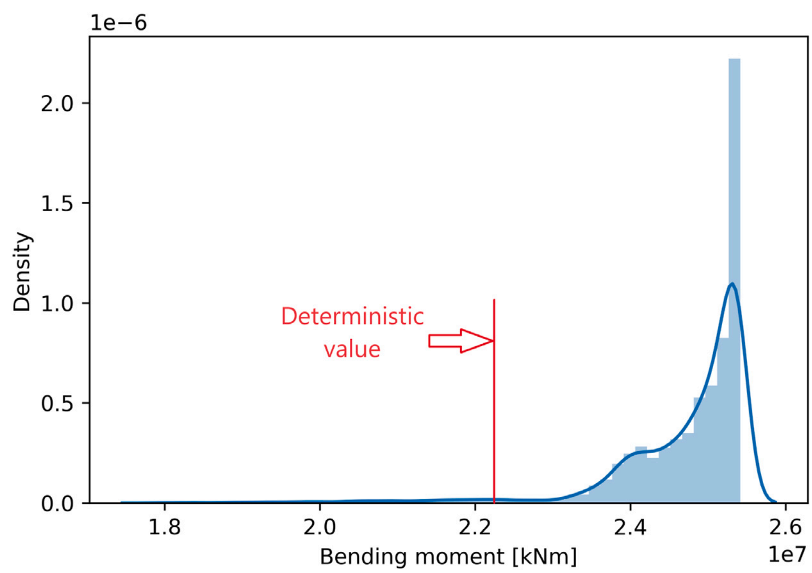

Fig. 13. Comparison of ultimate strength capacity: deterministic and probabilistic approach, collision-induced damage, hogging condition, VLCC tanker case.

information cannot be revealed using only a deterministic approach, where the values of ultimate capacity for both grounding and collision are quite similar.

3.2. Sensitivity analysis: Influence of considered corrosion model on ultimate strength

To obtain insights in the influence of the corrosion degradation model on the ultimate strength, five cases are considered, as follows:

- deterministic model, where corrosion is considered only as a deduction in thickness equal to half of the corrosion additions (current industry approach) $t_{corr} = t_{design} - 0.5t_c$ **(model 1)**;
- deterministic model, where corrosion is considered as a deduction in thickness of half of the corrosion additions (similar as above), with further consideration of the mean CF for each cross-section element to account for the loss of material and structural strength, deduced from Fig. 4 **(model 2)**;
- semi-probabilistic model, where corrosion is randomly distributed within a cross-section, accounting for the mean CF for each cross-section element, deduced from Fig. 4 **(model 3)**;
- semi-probabilistic model, where corrosion is considered as a deduction in thickness of half of the corrosion additions with randomly distributed CFs within cross-section elements, sampled from Fig. 4 **(model 4)**;
- fully probabilistic model (as described in Section 2.2) with randomly distributed corrosion deduction levels within cross-section with randomly distributed CFs considering uncertainty in its prediction (see Section 2.2) **(model 5)**.

For these sensitivity studies regarding the adopted corrosion model, the cross-section is considered to be undamaged. This allows to see the impact of different corrosion modelling approaches on the resulting ultimate strength without disturbance caused by the uncertainty that damage brings. An example of a histogram of the ultimate strength capacity of the VLCC tanker case considering the fully probabilistic model 5 for hogging conditions is presented in Fig. 15. It is noted that probability distribution follows normal probability distribution.

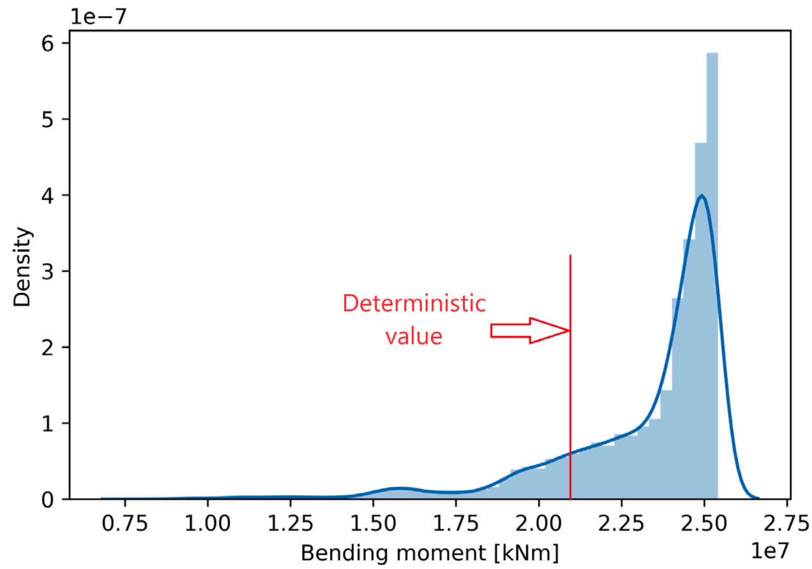

Fig. 14. Comparison of ultimate strength capacity: deterministic and probabilistic approach, grounding-induced damage, hogging condition, VLCC tanker case.

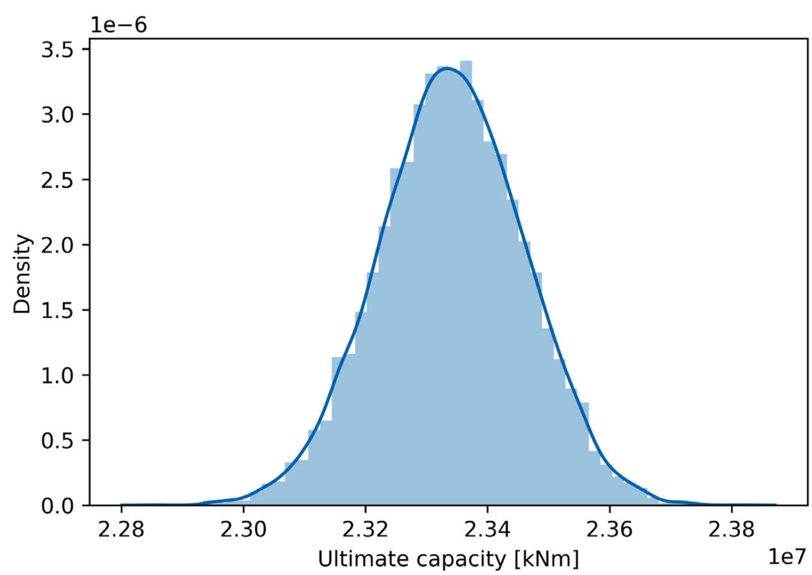

Fig. 15. Histogram of ultimate strength capacity, fully probabilistic corrosion model (model 5), hogging condition, VLCC tanker case.

For reasons of brevity, histograms showing the results of ultimate strength as per the other corrosion models are not provided here. Instead, a summary of the ultimate strength capacity results obtained for the different models is presented in Table 7. First, it is noted that there is a significant difference between deterministic models 1 and 2. This indicates that the ultimate capacity is significantly lower when the CF is considered, i.e. when the actual local effects of corrosion on the loss of material and structural strength are accounted for. Second, it is observed that when the uncertainty associated with the determination of the CF is considered, this has almost no impact on the resulting ultimate strength (see model 4), leading to a narrow standard deviation. Third, accounting for a random distribution of corrosion degradation levels within the cross-section (model 3) leads to a much higher effect on the uncertainty about the resulting ultimate strength. In this case, although the mean value is slightly higher compared to deterministic model 2, the minimum value is considerably lower compared to that model. Nevertheless, even in that case, the Standard Deviation is equal to 155 MN m in sagging (Coefficient of Variation is lower than 1%). Finally, when the fully probabilistic model is considered (model 5), which employs a superposition of uncertainties associated with corrosion loss in the cross-section elements and CF, the resulting ultimate strength distribution is similar to that obtained using model 3. In conclusion, it is found that the uncertainty about the ultimate strength capacity is dominated by the uncertainty associated with uneven corrosion levels within the cross-section. Nevertheless, the superposition of these two uncertainties (model 5, which corresponds to one described in Section 2.2) leads to obtaining the lowest minimum value within all considered models in the case of the hogging condition.

3.3. Framework application: Reliability analysis results for considered tanker design cases

The reliability analysis was performed as described in detail in Section 2.4. The degradation level was considered non-uniformly distributed within the cross-section as described in Section 2.2, corresponding to the corrosion level after 25 years of exploitation. The histograms of ultimate strength capacity for the fully probabilistic model accounting for damage extent (described in detail Section 2)

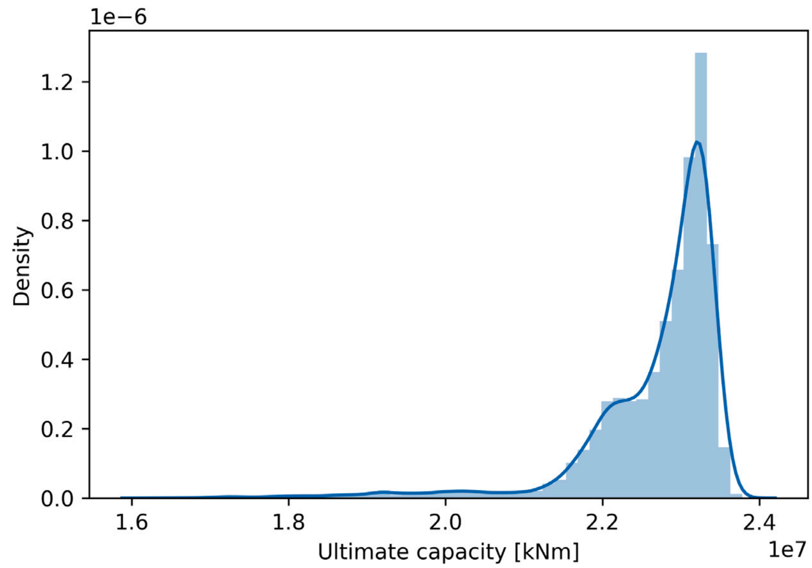

Fig. 16. Histogram of ultimate strength capacity, VLCC tanker, hogging condition, collision damage.

Table 7
Summary of ultimate strength calculated according to various corrosion models 1 to 5, VLCC tanker case.

Loading	Model no	Ultimate strength		
		Mean [MN m]	St. Dev. [MN m]	Min [MN m]
Sagging	1	19 800	–	–
	2	18 023	–	–
	3	18 164	155	17 555
	4	18 023	12.7	17 968
	5	18 161	156	17 569
Hogging	1	25 416	–	–
	2	23 206	–	–
	3	23 341	118	22 901
	4	23 206	11.3	23 160
	5	23 341	119	22 857

in hogging condition with damage due to collision are presented in Figs. 16 and 17 for VLCC and Handysize tanker, respectively.

The spread in ultimate strength capacity is higher in the case of a Handysize tanker compared to VLCC: for the former, the Coefficient of Variation (i.e. Standard Deviation divided by Mean value) is around 6%, whereas for the latter, this is around 4%. A plausible explanation for this observation is the different impact of the corrosion degradation between these cases. It is noted that although the mean thickness loss due to corrosion does not vary with the ship's length, the plating thickness and stiffener dimensions are much higher for VLCC. Thus, the plates for Handysize are relatively thinner, leading to higher DoD values, so the corrosion effect will be more severe, which leads to more severe effects on the strength reduction per structural element and on the overall ultimate hull girder strength.

It is observed that while the numerical values differ by an order of magnitude, both histograms have a similar shape, and do not follow any known probability distribution. Since in reliability analysis, a mathematical description of a probability distribution is required to enable calculating the ultimate capacity, the Kernel Density Estimation (KDE) method [97] is used to describe the probability density function (PDF). The PDFs estimated using KDE are shown in Figs. 16 and 17 as well. This is important since reliability analyses are generally sensitive to the so-called "tail-effect" [84]. If the most extreme values of the distribution (which are the ones mainly associated with failure, and in this case, correspond to the lowest ultimate strength capacity values) are modelled very roughly through the PDF, this can lead to significant uncertainty in the prediction of the probability of failure. In this view, KDE could show local extrema even in lower values of ultimate strength, whereas classical distributions are rather smooth in that region. The other random variables, i.e. those describing the still water bending moment, the wave bending moment, and their associated uncertainties, are accounted for as described in 2.4.

The method to calculate the probability of failure and corresponding reliability index applied in the current framework is chosen as Monte Carlo Simulations, as implemented in the UQ[py]lab toolbox [72]. The reason for this choice is that the ultimate capacity is estimated using KDE, given that the PDF does not follow any known shape associated with a closed-form mathematical expression. Thus, the sampling method is considered to be most appropriate. The number of generated samples for each reliability analysis calculation is taken as 1 million, based on convergence studies as shown in Fig. 18 for one of the analysed cases (Handysize tanker, grounding in hogging, ballast condition). In this figure, both the probability of failure (P_f) and the associated reliability index (β) are given in function of the number of samples, together with their respective confidence intervals. It is observed that from approx. 0.6 million samples, the values of P_f and β stabilize, and their confidence intervals are minimal.

The results of the reliability analysis for the two considered tanker design cases are presented in Table 8 for a range of scenarios, including intact (non-damaged hull) conditions. The probabilities of failure for both full load and ballast conditions are calculated based on the reliability analysis. The resulting P_f is calculated according to Eq. (24). The resulting reliability index β shown in the right column is calculated based on the resulting probability of failure using a well-known relationship [84]:

$$\beta = -\phi^{-1}(P_f) \tag{25}$$

It is observed that the most dangerous scenario for both ships is grounding in sagging conditions, where particularly full load conditions have the highest impact on the resulting reliability index. This is reasonable since, in the most serious grounding scenarios, a large cross-section area of the double bottom is reduced so that the deck region, which usually has weaker structural strength, will be subjected to high compression loads, which then lead to premature buckling and failure of the entire hull girder. In addition, the still water loads can, in this scenario, be significantly increased due to the flooding of ballast tanks, which are typically empty in full loading conditions. The obtained reliability indices in sagging conditions are lower for Handysize tankers, which can be explained by the effects of corrosion

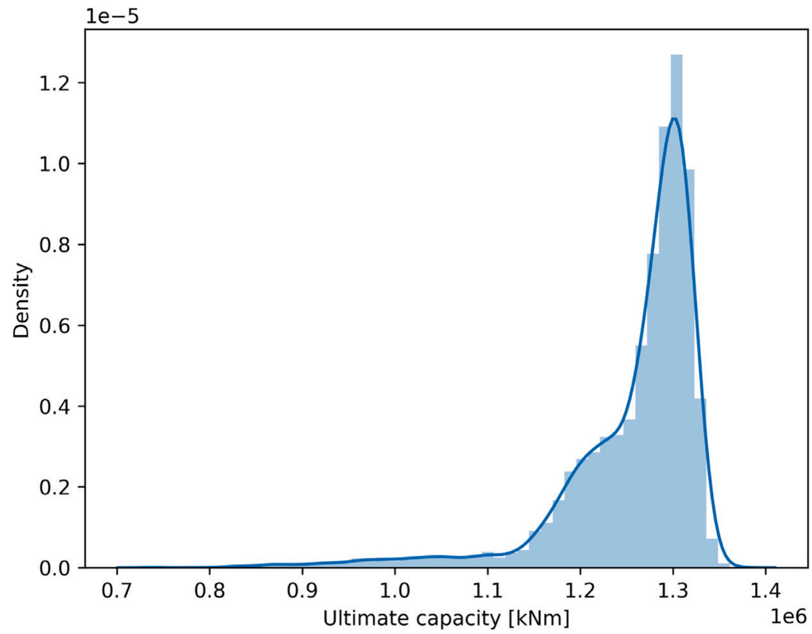

Fig. 17. Histogram of ultimate strength capacity, Handysize tanker, hogging condition, collision damage.

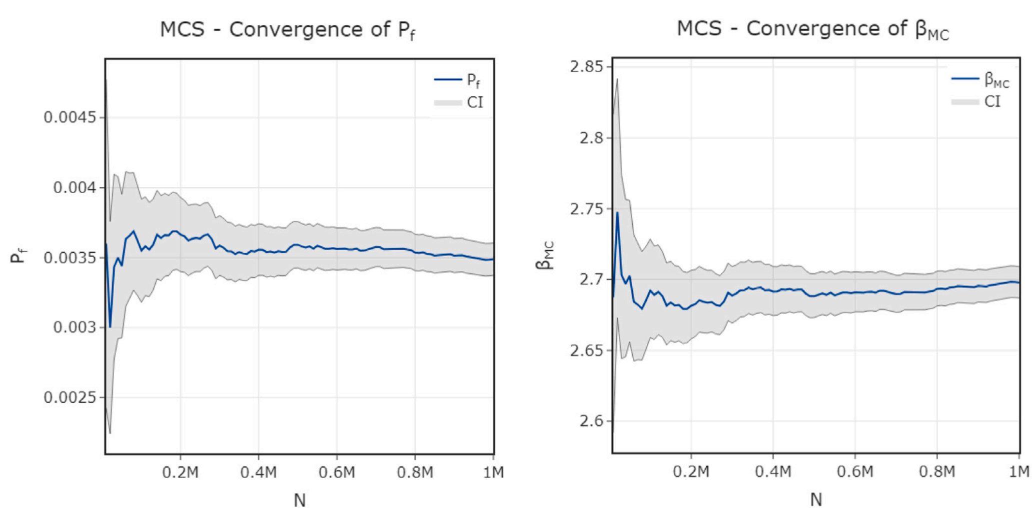

Fig. 18. Convergence test of the considered reliability method.

Table 8
Results of the reliability analysis for the VLCC and Handysize tanker cases, hogging and sagging, full load, ballast, and total lifetime conditions.

Ship	Scenario	Probability of failure [−]			β [−]
		Full load	Ballast	Resulting	
VLCC	Intact in sagg.	$2.58 \cdot 10^{-3}$	$8.20 \cdot 10^{-10}$	$1.03 \cdot 10^{-3}$	3.08
	Intact in hogg.	$2.90 \cdot 10^{-13}$	$4.00 \cdot 10^{-6}$	$1.60 \cdot 10^{-6}$	4.66
	Grounding in sagg.	$2.42 \cdot 10^{-2}$	$3.06 \cdot 10^{-3}$	$1.09 \cdot 10^{-2}$	2.29
	Grounding in hogg.	$3.10 \cdot 10^{-4}$	$2.18 \cdot 10^{-2}$	$8.85 \cdot 10^{-3}$	2.37
	Collision in sagg.	$8.16 \cdot 10^{-3}$	$2.86 \cdot 10^{-5}$	$3.27 \cdot 10^{-3}$	2.72
	Collision in hogg.	$1.11 \cdot 10^{-7}$	$1.70 \cdot 10^{-3}$	$6.81 \cdot 10^{-4}$	3.20
Handysize	Intact in sagg.	$1.95 \cdot 10^{-2}$	$1.31 \cdot 10^{-9}$	$7.81 \cdot 10^{-3}$	2.42
	Intact in hogg.	$2.94 \cdot 10^{-14}$	$8.85 \cdot 10^{-6}$	$3.54 \cdot 10^{-6}$	4.49
	Grounding in sagg.	$2.57 \cdot 10^{-2}$	$2.41 \cdot 10^{-3}$	$1.12 \cdot 10^{-2}$	2.28
	Grounding in hogg.	$1.20 \cdot 10^{-5}$	$3.49 \cdot 10^{-3}$	$1.40 \cdot 10^{-3}$	2.99
	Collision in sagg.	$2.09 \cdot 10^{-2}$	$2.51 \cdot 10^{-5}$	$8.37 \cdot 10^{-3}$	2.39
	Collision in hogg.	$2.24 \cdot 10^{-7}$	$2.63 \cdot 10^{-4}$	$1.05 \cdot 10^{-4}$	3.71

degradation, which brings higher variation in the ultimate strength capacity, as discussed at the beginning of this Section.

In contrast, the safest scenario for both tanker cases is the collision in hogging conditions. This is also a reasonable result since in such accidents, structural elements closer to the deck region are damaged, whereas the hull structure near the bottom remains intact. In hogging conditions, the bottom area carries high compression loads and, if intact, could resist buckling much longer. Finally, it is observed that the Handysize tanker hull girder is generally more prone to fail in sagging conditions, regardless of the damage type (even in intact conditions). In the VLCC tanker case, grounding damages are much more dangerous, regardless of the type of loading.

In the case of the VLCC tanker, the intact conditions are safer compared to damaged ones, even though significantly higher wave loads are considered. However, in the case of a Handysize tanker in sagging, the reliability index in intact conditions is very close to that in damaged conditions.

4. Discussion

As shown by [65], not considering the rotation of the neutral axis could result in an overestimation of the hull girder ultimate strength of up to 8%. Furthermore, it is emphasized that the iterative approach to predict the ultimate strength of ship hull girder is well-recognized as being accurate, as verified, for instance, in a benchmark study by ISSC (International Ships and Offshore Structures Committee) [99]. This study suggests that the iterative approach, in some cases, even outperforms advanced FE simulations. Although the latter approach seems to be the most advanced currently, it is still subjected to high uncertainty for the problems of ultimate strength, which showed a very recent study also done by ISSC [83]. There was a big spread in the participants' results because the FE simulations are sensitive to adopted modelling techniques, parameter settings and FE solvers. In the case of the iterative approach, the basic stress–strain curves of elements are calculated using pre-defined analytical equations, and only the division of cross-section into particular element types gives room for some uncertainties. Finally, FE analysis is highly time-consuming both in modelling and computational time, especially for large-scale objects such as ship sections. On the contrary, the iterative approach provides fast and reliable data and seems to be perfectly suited for probabilistic analysis, where multiple runs of computations are performed. Finally, in the presented study, only the Vertical Bending Moment was considered as an acting load. It is known that the Ultimate Limit State could consider both Vertical and Horizontal Bending moments (e.g. due to hull inclination during flooding). However, as was shown in [37], the most unfavourable loading conditions are where only Vertical Bending Moment is acting. Thus, from a safety perspective, considering only Vertical Bending Moment is sufficient.

The obtained hull girder failure probabilities presented in Table 8 can be considered very high, with a maximum value reaching approx. $1.1 \cdot 10^{-2}$ for both VLCC and Handysize tankers, which corresponds to a reliability index of 2.3. Nevertheless, those probabilities are associated with corrosion corresponding to 25 years of exploitation period. The probability of failure at the beginning of ship exploitation with no corrosion or very little corrosion will obviously be much smaller. However, it is also worth noting that even in intact condition, the reliability indices are quite low (especially for handysize tankers), showing the significant impact of corrosion degradation since no damage is considered in those cases. In the case of the handysize tanker, the reliability index for the intact condition was quite close to the damaged one due to much higher wave loads acting in the former. However, for the VLCC tanker, the intact conditions were much more favourable. Thus, the Handyszie tanker is designed in a more Risk-based manner.

There are no strict guidelines on what reliability index may be considered acceptable, but according to [100], the target failure probability level is equal to 10^{-4} for serious consequences and 10^{-3} for less serious consequences of failure. These probability values correspond to reliability indices $\beta = 3.71$ and $\beta = 3.09$, respectively. In the presented case studies, the possible consequences should be associated with the loss of the ship and a major oil spill, i.e. ecological catastrophe. Thus, there should be considered serious consequences and could be quantified in future studies with more sophisticated tools (e.g. [6,32,44,71]). In this view, the obtained reliability indices in current study appear to be much lower. It is noted that in a similar recently published study [62], in which an Aframax tanker ship was analysed (i.e. of medium size between VLCC and Handysize considered in the present work), a similar order of magnitude of P_f equal to $4 \cdot 10^{-2}$ for collision and $5 \cdot 10^{-2}$ for grounding were obtained, even with a simplified deterministic corrosion model adopted and having in mind that also several assumptions were made in that study. Thus, with consideration of CF and non-uniform corrosion spread, those values could be even higher. Based on this, the presented results seem to be rational but also concerning, if not alarming.

Some limitations of the current work should be highlighted. First, future work to account more accurately for the wave conditions and associated loads in the harbour and coastal areas should be considered to estimate the failure probability more accurately. Similarly, the uncertainties considered in ultimate strength computations, such as the assumption about the normal distribution of CF, should be revisited in further research.

Second, the presented study adopted the collision and grounding damage distributions as given in [74]. Although these statistics themselves can be considered rather reliable, there are some shortcomings to how the accidental damages are accounted for, which can have an effect on the accuracy of the findings of the current study. One such shortcoming is that the ship's age is not considered as a variable in the damage statistics. Since corrosion has an impact on structural crashworthiness, it is likely that in the same collision or grounding scenario, the damage extent will be more extensive for older ships compared to new ones. Thus, it could result in an even higher probability of failure for aged ships, whereas current statistics do not distinguish different ship ages. Another issue is that the statistics do not link the damage extent with the prevailing loading conditions during the accident. For example, it is plausibly more likely that a grounding is suffered during a voyage in full load condition than in ballast since, in the latter case, the draught of the ship is significantly smaller. A further limitation of the accident scenarios, which has also been highlighted in [41], is that these do not account for the impact conditions, such as the vessel speed or impact angle, whereas these factors have a significant impact on the energy dissipation and damage extent. As in harbour and coastal areas, the vessel speeds when collision and grounding impacts occur are lower than in open water areas [101]. Understanding this relation to accident statistics better can also improve the estimation of the hull girder failure probability. A final limiting aspect of how the accidental damage is accounted for in the current work is that these do not account for different structural configurations or crashworthiness optimization, whereas it is known that these can have significant effects on the damage sustained by the ship hull [35,47]. Therefore, more research is needed to better understand the accident conditions, linking hull damages with loading scenarios, ship age, and hull configuration. Future work can be directed to using more explicit methods for collision and grounding damage assessment, along with advanced statistical methods, to improve the accuracy of this damage modelling and estimation [36].

Apart from the above described limitations, some directions for future research can be suggested. For instance, in the current state-of-art of risk-based ship design for ice-classed vessels [2], some attention has been given to the effects of corrosion on the ultimate and accidental strength [102,103]. A more detailed consideration of advanced corrosion degradation models in relation to local ice loads on the ship hull, and on the associated risk of subsequent consequences such as flooding, hull girder failure and/or environmental damage, can improve the current understanding of the safety level of vessels operating in Arctic and ice-covered waters. Another avenue for future work concerns the use of advanced models for accidental damage and hull girder failure considering corrosion degradation, as presented in this article, for analysing the risk of the maritime transportation system in specific geographical areas, extending frameworks such as [28,32]. Such work can advance waterway risk management, for instance, related to improved marine pollution preparedness and response planning and risk management decision making [11,33] and improved maritime Search and Rescue preparedness planning, e.g. extending methods such as [104].

Finally, although the presented method focuses to serve for risk-based ship design, it has the potential to be used for condition assessment of existing structures. This can be especially useful since the commonly adopted 25-year exploitation period can be extended, especially in lucrative shipping markets and as a response to new regulation [105]. Thus, the impact of corrosion on the probability of hull girder failure for significantly aged ships is an important issue, but the associated risk is not accurately understood for older vessels. Earlier presented deterministic analysis results for a 50-year old hull [52] indicate that the rule criteria are not satisfied anymore, indicating that ageing significantly increases the probability of hull failure. Therefore, feeding the proposed framework with inspection data, accounting for relevant uncertainties, can be useful to quantify the risk level and associated safety margins of an existing ship structure. This can be a fruitful direction for future research and development, possibly linked with other contemporary developments such as digital twinning of ship structures [106].

5. Conclusions

This article proposes a novel probabilistic framework to analyse the probability of ship hull girder failure, accounting for advanced corrosion degradation modelling and accidental damage. This framework presents a meaningful step forward in developing methods and tools to advance the risk-based ship design paradigm into practical application. In this paradigm, ship structures are designed based on an explicit consideration of the probability of all possible loads and associated risks to which a vessel is exposed over the whole target exploitation period, including accidents in maritime traffic. For this purpose, the effects of ship ageing, in which corrosion is among the most prominent factors, cannot be excluded. Hence, state-of-the-art methods and approaches from corrosion degradation modelling should be incorporated in risk-based ship design frameworks.

The major contributions of the proposed framework and the executed case studies can be summarized as follows:

- The iterative approach for calculating the ultimate strength, which is a fast and reliable method as confirmed by validation with available experiments, is incorporated in the framework;
- A novel approach for corrosion degradation modelling is adopted, which consists of random sampling from a distribution of degradation levels within the ship's cross-section and accounts for the decrease in strength caused by the non-uniform distribution of thickness in the structural elements composing the cross-section. This is calculated by introducing a Correction Factor and the associated uncertainties.
- Sensitivity studies for a VLCC tanker case and results of a reliability analysis for tanker cases show that incorporating such a method to account for the local effects of corrosion degradation on ultimate strength analysis and risk-based design is of high importance;
- The extent of accidental damage is considered probabilistically, and when superimposed with corrosion effects, the associated uncertainty about damage size can lead to a significant failure probability. While some assumptions in the case studies may contribute to finding such probabilities of hull failure, these results raise concern, especially considering that other recent studies lead to similar conclusions. The consequences of failure should be associated with the loss of the ship and a major oil spill. This is found regardless of the ship size, with an even higher probability obtained for the Handysize tanker case;
- The importance of considering proper corrosion degradation modelling is also presented by calculating the failure probability for intact (i.e. non-damaged conditions), where for both case studies, resulting reliability was lower than the target reliability index for serious consequences of failure;
- The developed framework is implemented using Python software, including reliability analysis using UQ[py]lab project consisting of state-of-the-art methods in uncertainty quantification and structural risk engineering. Correspondingly, there is no need to build an interface between different software, including commercial ones, so that further development of the framework can be easily pursued, which in turn can further advance risk-based ship design practices.

Notwithstanding the above-listed achievements, the presented framework still has some limitations and drawbacks, as discussed in Section 4. These mainly relate to the modelling of still water and wave loads, and improving the understanding of the conditions under which accidents occur, in terms of the ship age, loading conditions, prevailing wave conditions, the ship's corrosion degradation condition, hull configuration and crashworthiness, and impact speeds and angles. Along with some other avenues for future work, these limitations can be fruitful areas for future research and development. Those are planned to be overcomed by integrating the presented tool with accident probability models and consequence models, heading towards a full physics-based, risk-based ship design framework.

CRediT authorship contribution statement

Krzysztof Woloszyk: Writing – review & editing, Writing – original draft, Visualization, Validation, Software, Methodology, Investigation, Formal analysis, Conceptualization. **Floris Goerlandt:** Writing – review & editing, Writing – original draft, Conceptualization. **Jakub Montewka:** Writing – review & editing, Conceptualization.

Declaration of competing interest

The authors declare that they have no known competing financial interests or personal relationships that could have appeared to influence the work reported in this paper.

Data availability

Data will be made available on request.

Acknowledgements

The first author greatly acknowledges the support of the Foundation for Polish Science (FNP), Poland.

The contributions by the second author have been made under the Qanittaq Clean Arctic Shipping Initiative project, financially supported by the Canada First Research Excellence Fund, Canada. Further support was received from the National Sciences and Engineering Research Council of Canada (NSERC) through the Canada Research Chairs Program, under grant CRC-2018-00110.

The third author acknowledges financial support received from the research grant funded by the Gdańsk University of Technology IDUB Americium International Career Development contract no. DEC-10/2023/IDU/II.1/AMERICIUM. Further funding was provided by Interreg Baltic Sea Region (co-funded by EU) via OpenRiskII project "Tool for shared and dynamic maritime traffic risk picture of the Baltic Sea Region" under grant No #C041.

References

[1] Papanikolaou A. Risk-based ship design. Berlin, Heidelberg: Springer Berlin Heidelberg; 2009, http://dx.doi.org/10.1007/978-3-540-89042-3.

[2] Kujala P, Goerlandt F, Way B, Smith D, Yang M, Khan F, Veitch B. Review of risk-based design for ice-class ships. Mar Struct 2019;63:181–95. http://dx.doi.org/10.1016/j.marstruc.2018.09.008.

[3] Pedersen PT. Review and application of ship collision and grounding analysis procedures. Mar Struct 2010;23(3):241–62. http://dx.doi.org/10.1016/j.marstruc.2010.05.001.

[4] Eliopoulou E, Alissafaki A, Papanikolaou A. Statistical analysis of accidents and review of safety level of passenger ships. J Mar Sci Eng 2023;11(2):410. http://dx.doi.org/10.3390/jmse11020410.

[5] Eliopoulou E, Papanikolaou A, Voulgarellis M. Statistical analysis of ship accidents and review of safety level. Saf Sci 2016;85:282–92. http://dx.doi.org/10.1016/j.ssci.2016.02.001.

[6] Ventikos NP, Sotiropoulos FS. Disutility analysis of oil spills: Graphs and trends. Mar Pollut Bull 2014;81(1):116–23. http://dx.doi.org/10.1016/j.marpolbul.2014.02.007.

[7] Lecklin T, Ryömä R, Kuikka S. A Bayesian network for analyzing biological acute and long-term impacts of an oil spill in the gulf of Finland. Mar Pollut Bull 2011;62(12):2822–35. http://dx.doi.org/10.1016/j.marpolbul.2011.08.045.

[8] Mazaheri A, Montewka J, Kujala P. Towards an evidence-based probabilistic risk model for ship-grounding accidents. Saf Sci 2016;86:195–210. http://dx.doi.org/10.1016/j.ssci.2016.03.002.

[9] Puisa R, McNay J, Montewka J. Maritime safety: Prevention versus mitigation? Saf Sci 2021;136:105151. http://dx.doi.org/10.1016/j.ssci.2020.105151.
[10] Fetissov M, Aps R, Goerlandt F, Jänes H, Kotta J, Kujala P, Szava-Kovats R. Next-generation smart response web (NG-SRW): An operational spatial decision support system for maritime oil spill emergency response in the gulf of Finland (Baltic Sea). Sustainability 2021;13(12):6585. http://dx.doi.org/10.3390/su13126585.
[11] Laine V, Goerlandt F, Banda OV, Baldauf M, Koldenhof Y, Rytkönen J. A risk management framework for maritime pollution preparedness and response: Concepts, processes and tools. Mar Pollut Bull 2021;171:112724. http://dx.doi.org/10.1016/j.marpolbul.2021.112724.
[12] Gil M, Wróbel K, Montewka J, Goerlandt F. A bibliometric analysis and systematic review of shipboard decision support systems for accident prevention. Saf Sci 2020;128:104717. http://dx.doi.org/10.1016/j.ssci.2020.104717.
[13] Ozturk U, Cicek K. Individual collision risk assessment in ship navigation: A systematic literature review. Ocean Eng 2019;180:130–43. http://dx.doi.org/10.1016/j.oceaneng.2019.03.042.
[14] Chen P, Huang Y, Mou J, van Gelder P. Probabilistic risk analysis for ship-ship collision: State-of-the-art. Saf Sci 2019;117:108–22. http://dx.doi.org/10.1016/j.ssci.2019.04.014.
[15] Du L, Goerlandt F, Kujala P. Review and analysis of methods for assessing maritime waterway risk based on non-accident critical events detected from AIS data. Reliab Eng Syst Saf 2020;200:106933. http://dx.doi.org/10.1016/j.ress.2020.106933.
[16] Zhang J, Jin M, Wan C, Dong Z, Wu X. A Bayesian network-based model for risk modeling and scenario deduction of collision accidents of inland intelligent ships. Reliab Eng Syst Saf 2024;243:109816. http://dx.doi.org/10.1016/j.ress.2023.109816.
[17] Shiokari M, Itoh H, Yuzui T, Ishimura E, Miyake R, Kudo J, Kawashima S. Structure model-based hazard identification method for autonomous ships. Reliab Eng Syst Saf 2024;247:110046. http://dx.doi.org/10.1016/j.ress.2024.110046.
[18] Zhang W, Zhang Y, Zhang C. Research on risk assessment of maritime autonomous surface ships based on catastrophe theory. Reliab Eng Syst Saf 2024;244:109946. http://dx.doi.org/10.1016/j.ress.2024.109946.
[19] Rong H, Teixeira A, Guedes Soares C. A framework for ship abnormal behaviour detection and classification using AIS data. Reliab Eng Syst Saf 2024;247:110105. http://dx.doi.org/10.1016/j.ress.2024.110105.
[20] Sotiralis P, Ventikos N, Hamann R, Golyshev P, Teixeira A. Incorporation of human factors into ship collision risk models focusing on human centred design aspects. Reliab Eng Syst Saf 2016;156:210–27. http://dx.doi.org/10.1016/j.ress.2016.08.007.
[21] Montewka J, Goerlandt F, Innes-Jones G, Owen D, Hifi Y, Puisa R. Enhancing human performance in ship operations by modifying global design factors at the design stage. Reliab Eng Syst Saf 2017;159:283–300. http://dx.doi.org/10.1016/j.ress.2016.11.009.
[22] Valdez Banda OA, Goerlandt F, Kuzmin V, Kujala P, Montewka J. Risk management model of winter navigation operations. Mar Pollut Bull 2016;108(1–2):242–62. http://dx.doi.org/10.1016/j.marpolbul.2016.03.071.
[23] Martins MR, Maturana MC. Application of Bayesian belief networks to the human reliability analysis of an oil tanker operation focusing on collision accidents. Reliab Eng Syst Saf 2013;110:89–109. http://dx.doi.org/10.1016/j.ress.2012.09.008.
[24] Zhang M, Kujala P, Hirdaris S. A machine learning method for the evaluation of ship grounding risk in real operational conditions. Reliab Eng Syst Saf 2022;226:108697. http://dx.doi.org/10.1016/j.ress.2022.108697.
[25] Akhtar MJ, Utne IB. Human fatigue's effect on the risk of maritime groundings – A Bayesian network modeling approach. Saf Sci 2014;62:427–40. http://dx.doi.org/10.1016/j.ssci.2013.10.002.
[26] Hussein A, El-Dessouky U, El-Kilani H, Hegazy E. Grounding contingency plan for intact double hull tanker. Alexandria Eng J 2016;55(1):235–41. http://dx.doi.org/10.1016/j.aej.2015.10.017.
[27] Renn O, Klinke A, van Asselt M. Coping with complexity, uncertainty and ambiguity in risk governance: A synthesis. Ambio 2011;40(2):231–46. http://dx.doi.org/10.1007/s13280-010-0134-0.
[28] Montewka J, Ehlers S, Goerlandt F, Hinz T, Tabri K, Kujala P. A framework for risk assessment for maritime transportation systems—A case study for open sea collisions involving RoPax vessels. Reliab Eng Syst Saf 2014;124:142–57. http://dx.doi.org/10.1016/j.ress.2013.11.014.
[29] Ruponen P, Montewka J, Tompuri M, Manderbacka T, Hirdaris S. A framework for onboard assessment and monitoring of flooding risk due to open watertight doors for passenger ships. Reliab Eng Syst Saf 2022;226:108666. http://dx.doi.org/10.1016/j.ress.2022.108666.
[30] Zhou K, Xing W, Wang J, Li H, Yang Z. A data-driven risk model for maritime casualty analysis: A global perspective. Reliab Eng Syst Saf 2024;244:109925. http://dx.doi.org/10.1016/j.ress.2023.109925.
[31] Wu B, Tang Y, Yan X, Guedes Soares C. Bayesian network modelling for safety management of electric vehicles transported in RoPax ships. Reliab Eng Syst Saf 2021;209:107466. http://dx.doi.org/10.1016/j.ress.2021.107466.
[32] Goerlandt F, Montewka J. A framework for risk analysis of maritime transportation systems: A case study for oil spill from tankers in a ship–ship collision. Saf Sci 2015;76:42–66. http://dx.doi.org/10.1016/j.ssci.2015.02.009.
[33] Parviainen T, Goerlandt F, Helle I, Haapasaari P, Kuikka S. Implementing Bayesian networks for ISO 31000:2018-based maritime oil spill risk management: State-of-art, implementation benefits and challenges, and future research directions. J Environ Manag 2021;278:111520. http://dx.doi.org/10.1016/j.jenvman.2020.111520.
[34] Otto S, Pedersen PT, Samuelides M, Sames PC. Elements of risk analysis for collision and grounding of a RoRo passenger ferry. Mar Struct 2002;15(4–5):461–74. http://dx.doi.org/10.1016/S0951-8339(02)00014-X.
[35] Klanac A, Varsta P. Design of marine structures with improved safety for environment. Reliab Eng Syst Saf 2011;96(1):75–90. http://dx.doi.org/10.1016/j.ress.2010.06.016.
[36] Liu B, Pedersen PT, Zhu L, Zhang S. Review of experiments and calculation procedures for ship collision and grounding damage. Mar Struct 2018;59:105–21. http://dx.doi.org/10.1016/j.marstruc.2018.01.008.
[37] Kuznecovs A, Schreuder M, Ringsberg JW. Methodology for the simulation of a ship's damage stability and ultimate strength conditions following a collision. Mar Struct 2021;79:103027. http://dx.doi.org/10.1016/j.marstruc.2021.103027.
[38] Liu B, Villavicencio R, Pedersen PT, Guedes Soares C. Analysis of structural crashworthiness of double-hull ships in collision and grounding. Mar Struct 2021;76:102898. http://dx.doi.org/10.1016/j.marstruc.2020.102898.
[39] Le Sourne H, Besnard N, Cheylan C, Buannic N. A ship collision analysis program based on upper bound solutions and coupled with a large rotational ship movement analysis tool. J Appl Math 2012;2012:1–27. http://dx.doi.org/10.1155/2012/375686.
[40] Tan X, Tao J, Konovessis D. Preliminary design of a tanker ship in the context of collision-induced environmental-risk-based ship design. Ocean Eng 2019;181:185–97. http://dx.doi.org/10.1016/j.oceaneng.2019.04.003.
[41] Ståhlberg K, Goerlandt F, Ehlers S, Kujala P. Impact scenario models for probabilistic risk-based design for ship–ship collision. Mar Struct 2013;33:238–64. http://dx.doi.org/10.1016/j.marstruc.2013.06.006.
[42] Zhang M, Conti F, Le Sourne H, Vassalos D, Kujala P, Lindroth D, Hirdaris S. A method for the direct assessment of ship collision damage and flooding risk in real conditions. Ocean Eng 2021;237:109605. http://dx.doi.org/10.1016/j.oceaneng.2021.109605.
[43] Tavakoli MT, Amdahl J, Leira BJ. Analytical and numerical modelling of oil spill from a side tank with collision damage. Ships Offshore Struct 2012;7(1):73–86. http://dx.doi.org/10.1080/17445302.2010.537844.
[44] Goerlandt F, Montewka J. A probabilistic model for accidental cargo oil outflow from product tankers in a ship–ship collision. Mar Pollut Bull 2014;79(1–2):130–44. http://dx.doi.org/10.1016/j.marpolbul.2013.12.026.
[45] Tabri K, Heinvee M, Laanearu J, Kollo M, Goerlandt F. An online platform for rapid oil outflow assessment from grounded tankers for pollution response. Mar Pollut Bull 2018;135:963–76. http://dx.doi.org/10.1016/j.marpolbul.2018.06.039.
[46] Haris S, Amdahl J. Analysis of ship–ship collision damage accounting for bow and side deformation interaction. Mar Struct 2013;32:18–48. http://dx.doi.org/10.1016/j.marstruc.2013.02.002.
[47] Hogström P, Ringsberg JW. Assessment of the crashworthiness of a selection of innovative ship structures. Ocean Eng 2013;59:58–72. http://dx.doi.org/10.1016/j.oceaneng.2012.12.024.
[48] Tabri K, Matusiak J, Varsta P. Sloshing interaction in ship collisions—An experimental and numerical study. Ocean Eng 2009;36(17–18):1366–76. http://dx.doi.org/10.1016/j.oceaneng.2009.08.017.
[49] Tabri K, Goerlandt F, Kujala P. Influence of compressive ice force in bow-to-aft ship collision. In: Cho S, Shin H, Choung J, Jung R, editors. Proceedings of the international conference on collision and grounding of ships and offshore structures. Ulsan, Korea: Society of Naval Architects of Korea; 2016.
[50] Ringsberg J, Kuznecovs A, Johnson E. Analysis of how the conditions in a collision scenario affect the size of a struck vessel's damage opening and ultimate strength. In: Ringsberg J, Guedes Soares C, editors. Advances in the analysis and design of marine structures. London: CRC Press; 2023, p. 639–47. http://dx.doi.org/10.1201/9781003399759-71.
[51] Antão P, Sun S, Teixeira A, Guedes Soares C. Quantitative assessment of ship collision risk influencing factors from worldwide accident and fleet data. Reliab Eng Syst Saf 2023;234:109166. http://dx.doi.org/10.1016/j.ress.2023.109166.
[52] Woloszyk K, Goerlandt F, Montewka J. A methodology for ultimate strength assessment of ship hull girder accounting for enhanced corrosion degradation modelling. Mar Struct 2024;93:103530. http://dx.doi.org/10.1016/j.marstruc.2023.103530.
[53] Liu B, Garbatov Y, Zhu L, Guedes Soares C. Numerical assessment of the structural crashworthiness of corroded ship hulls in stranding. Ocean Eng 2018;170:276–85. http://dx.doi.org/10.1016/j.oceaneng.2018.10.034.
[54] Rata V, Rusu L. Assessing the traffic risk along the main black sea maritime routes. In: Proceedings of international conference on traffic and transport engineering. Belgrade, Serbia; 2018, p. 290–7.

[55] Rata V, Rusu L. Assess the risk of shipping accidents in the black sea that may be based on structural damage. In: Proceedings of 1st international conference of maritime science & technology nase more. Dubrovnik, Croatia; 2019.
[56] INTERCARGO. Bulk carrier casualty report. Years 2010 to 2019 and trends. Tech. rep., International Association of Dry Cargo Shipowners; 2020.
[57] Moan T, Ayala-Uraga E. Reliability-based assessment of deteriorating ship structures operating in multiple sea loading climates. Reliab Eng Syst Saf 2008;93(3):433–46. http://dx.doi.org/10.1016/j.ress.2006.12.008.
[58] Gong C, Frangopol DM. Time-variant hull girder reliability considering spatial dependence of corrosion growth, geometric and material properties. Reliab Eng Syst Saf 2020;193:106612. http://dx.doi.org/10.1016/j.ress.2019.106612.
[59] Liu Y, Frangopol DM. Time-dependent reliability assessment of ship structures under progressive and shock deteriorations. Reliab Eng Syst Saf 2018;173:116–28. http://dx.doi.org/10.1016/j.ress.2018.01.009.
[60] Li H, Guedes Soares C. Assessment of failure rates and reliability of floating offshore wind turbines. Reliab Eng Syst Saf 2022;228:108777. http://dx.doi.org/10.1016/j.ress.2022.108777.
[61] Hussein A, Guedes Soares C. Reliability and residual strength of double hull tankers designed according to the new IACS common structural rules. Ocean Eng 2009;36(17–18):1446–59. http://dx.doi.org/10.1016/j.oceaneng.2009.04.006.
[62] Bužančić Primorac B, Parunov J, Guedes Soares C. Structural reliability analysis of ship hulls accounting for collision or grounding damage. J Mar Sci Appl 2020;19(4):717–33. http://dx.doi.org/10.1007/s11804-020-00176-w.
[63] Yao T, Fujikubo M. Buckling and ultimate strength of ship and ship-like floating structures. Elsevier; 2016.
[64] Woloszyk K, Montewka J, Goerlandt F. A simplified method to assess the impact of ship-to-ship collision on the risk of tanker ship hull girder breaking accounting for the effect of ageing. In: Advances in the collision and grounding of ships and offshore structures. London: CRC Press; 2023, p. 413–9. http://dx.doi.org/10.1201/9781003462170-50.
[65] Fujikubo M, Zubair Muis Alie M, Takemura K, Iijima K, Oka S. Residual hull girder strength of asymmetrically damaged ships. J Japan Soc Nav Archit Ocean Eng 2012;16:131–40. http://dx.doi.org/10.2534/jjasnaoe.16.131.
[66] Garbatov Y, Guedes Soares C, Parunov J, Kodvanj J. Tensile strength assessment of corroded small scale specimens. Corros Sci 2014;85:296–303. http://dx.doi.org/10.1016/j.corsci.2014.04.031.
[67] Woloszyk K, Garbatov Y. An enhanced method in predicting tensile behaviour of corroded thick steel plate specimens by using random field approach. Ocean Eng 2020;213:107803. http://dx.doi.org/10.1016/j.oceaneng.2020.107803.
[68] Piscopo V, Scamardella A. Incidence of pitting corrosion wastage on the hull girder ultimate strength. J Mar Sci Appl 2021;20(3):477–90. http://dx.doi.org/10.1007/s11804-021-00218-x.
[69] Bužančić Primorac B, Slapničar V, Munić I, Grubišić V, Ćorak M, Parunov J. Statistics of still water bending moment of damaged suezmax oil tanker. In: M. Altosole A Francescutto, editor. Proceedings of the 18th international conference on ships and shipping research, organising committee NAV 2015. Lecco, Italy; 2015, p. 580–9.
[70] Rodrigues J, Teixeira A, Guedes Soares C. Probabilistic analysis of the hull-girder still water loads on a shuttle tanker in full load condition, for parametrically distributed collision damage spaces. Mar Struct 2015;44:101–24. http://dx.doi.org/10.1016/j.marstruc.2015.08.002.
[71] Montewka J, Goerlandt F, Zheng X. Probabilistic meta-models evaluating accidental oil spill size from tankers. In: Weintrit A, Neumann T, editors. Maritime pollution and environment protection. CRC Press; 2015, p. 231–41.
[72] Lataniotis C, Marelli S, Sudret B. Uncertainty quantification in the cloud with uqcloud. In: Proceedings of the 4thInternational conference on uncertainty quantification in computational sciences and engineering. UNCECOMP2021, Athens, Greece; 2021.
[73] IACS. Common structural rules for bulk carriers and oil tankers. 2023.
[74] International Maritime Organization. Revised interim guidelines for the approval of alternative methods of design and construction of oil tankers under regulation 13f(5) of annex I of MARPOL 73/78. 2003.
[75] Olsson A, Sandberg G, Dahlblom O. On latin hypercube sampling for structural reliability analysis. Struct Saf 2003;25(1):47–68. http://dx.doi.org/10.1016/S0167-4730(02)00039-5.
[76] Saad-Eldeen S, Garbatov Y, Guedes Soares C. Ultimate strength assessment of corroded box girders. Ocean Eng 2013;58:35–47. http://dx.doi.org/10.1016/j.oceaneng.2012.09.019.
[77] Woloszyk K, Garbatov Y. Advanced numerical modelling for predicting residual compressive strength of corroded stiffened plates. Thin-Walled Struct 2023;183:110380. http://dx.doi.org/10.1016/j.tws.2022.110380.
[78] Woloszyk K, Garbatov Y, Kowalski J. Experimental ultimate strength assessment of stiffened plates subjected to marine immersed corrosion. Appl Ocean Res 2023;138:103679. http://dx.doi.org/10.1016/j.apor.2023.103679.
[79] Ivosevic S, Mestrovic R, Kovac N. Probabilistic estimates of corrosion rate of fuel tank structures of aging bulk carriers. Int J Nav Archit Ocean Eng 2019;11(1):165–77. http://dx.doi.org/10.1016/j.ijnaoe.2018.03.003.
[80] IACS. Harmonised CSR TB report: corrosion additions and wastage allowances. Tech. rep., London; 2018.
[81] Smith S. Influence of local compressive failure on ultimate longitudinal strength of a ship's hull. In: Proc. int. sym. on practical design in shipbuilding. 1977, p. 73–9.
[82] Komoriyama Y, Tanaka Y, Ando T, Hashizume Y, Tatsumi A, Fujikubo M. Ultimate longitudinal bending strength of damaged box girder in upright and inclined conditions – model experiment and numerical analysis. In: Advances in the collision and grounding of ships and offshore structures. London: CRC Press; 2023, p. 377–85. http://dx.doi.org/10.1201/9781003462170-46.
[83] Ringsberg JW, Darie I, Nahshon K, Shilling G, Vaz MA, Benson S, Brubak L, Feng G, Fujikubo M, Gaiotti M, Hu Z, Jang B-S, Paik J-K, Slagstad M, Tabri K, Wang Y, Wiegard B, Yanagihara D. The issc 2022 committee iii.1-ultimate strength benchmark study on the ultimate limit state analysis of a stiffened plate structure subjected to uniaxial compressive loads. Mar Struct 2021;79:103026. http://dx.doi.org/10.1016/j.marstruc.2021.103026.
[84] Ditlevsen O, Madsen HO. Structural reliability methods. Chichester: John Wiley and Sons; 1996.
[85] Aven T. On the use of conservatism in risk assessments. Reliab Eng Syst Saf 2016;146:33–8. http://dx.doi.org/10.1016/j.ress.2015.10.011.
[86] Park I, Amarchinta HK, Grandhi RV. A Bayesian approach for quantification of model uncertainty. Reliab Eng Syst Saf 2010;95(7):777–85. http://dx.doi.org/10.1016/j.ress.2010.02.015.
[87] Li S, Kim DK, Ringsberg J, Liu B, Benson S. Uncertainty of ship hull girder ultimate strength in longitudinal bending. Int J Marit Eng 2022;164(A2):185–206. http://dx.doi.org/10.5750/ijme.v164iA2.1157.
[88] Guedes Soares C, Teixeira A. Structural reliability of two bulk carrier designs. Mar Struct 2000;13(2):107–28. http://dx.doi.org/10.1016/S0951-8339(00)00004-6.
[89] Garbatov Y, Sisci F, Ventura M. Risk-based framework for ship and structural design accounting for maintenance planning. Ocean Eng 2018;166:12–25. http://dx.doi.org/10.1016/j.oceaneng.2018.07.058.
[90] Luís R, Teixeira A, Guedes Soares C. Longitudinal strength reliability of a tanker hull accidentally grounded. Struct Saf 2009;31(3):224–33. http://dx.doi.org/10.1016/j.strusafe.2008.06.005.
[91] Jia H, Moan T. Reliability analysis of oil tankers with collision damage. In: Volume 2: structures, safety and reliability, ASMEDC. 2008, p. 55–63. http://dx.doi.org/10.1115/OMAE2008-57102.
[92] Guedes Soares C, Dogliani M, Ostergaard C, Parmentier G, Pedersen PT. Reliability based ship structural design. Trans Soc Nav Archit Mar Eng (SNAME) 1996;104:359–89.
[93] Munim ZH, Sørli MA, Kim H, Alon I. Predicting maritime accident risk using automated machine learning. Reliab Eng Syst Saf 2024;110148. http://dx.doi.org/10.1016/j.ress.2024.110148.
[94] Rawson A, Sabeur Z, Brito M. Intelligent geospatial maritime risk analytics using the discrete global grid system. Big Earth Data 2022;6(3):294–322. http://dx.doi.org/10.1080/20964471.2021.1965370.
[95] Woloszyk K, Garbatov Y. Structural reliability assessment of corroded tanker ship based on experimentally estimated ultimate strength. Polish Marit Res 2019;26(2):47–54. http://dx.doi.org/10.2478/pomr-2019-0024.
[96] Albaigés J, Morales-Nin B, Vilas F. The prestige oil spill: A scientific response. Mar Pollut Bull 2006;53(5–7):205–7. http://dx.doi.org/10.1016/j.marpolbul.2006.03.012.
[97] Rosenblatt M. Remarks on some nonparametric estimates of a density function. Ann Math Stat 1956;27(3):832–7. http://dx.doi.org/10.1214/aoms/1177728190.
[98] Lone EN, Sauder T, Larsen K, Leira BJ. Probabilistic fatigue model for design and life extension of mooring chains, including mean load and corrosion effects. Ocean Eng 2022;245:110396. http://dx.doi.org/10.1016/j.oceaneng.2021.110396.
[99] Paik JK, Amlashi H, Boon B, Branner K, Caridis P, Das P, Fujikubo M, Huang C-H, Josefson L, Kaeding P, et al. Committee iii. 1 ultimate strength. In: 18th international ship and offshore structures congress. 2012, p. 285–363.
[100] DNV. Structural reliability analysis of marine structures. Classification notes No 30.6, 1992.
[101] Goerlandt F, Ståhlberg K, Kujala P. Influence of impact scenario models on collision risk analysis. Ocean Eng 2012;47:74–87. http://dx.doi.org/10.1016/j.oceaneng.2012.03.006.
[102] Park DK, Kim DK, Seo JK, Kim BJ, Ha YC, Paik JK. Operability of non-ice class aged ships in the Arctic ocean—Part I: Ultimate limit state approach. Ocean Eng 2015;102:197–205. http://dx.doi.org/10.1016/j.oceaneng.2014.12.040.
[103] Park DK, Kim DK, Seo JK, Kim BJ, Ha YC, Paik JK. Operability of non-ice class aged ships in the Arctic ocean-part II: Accidental limit state approach. Ocean Eng 2015;102:206–15. http://dx.doi.org/10.1016/j.oceaneng.2015.04.038.
[104] Akbari A, Pelot R, Eiselt HA. A modular capacitated multi-objective model for locating maritime search and rescue vessels. Ann Oper Res 2018;267(1–2):3–28. http://dx.doi.org/10.1007/s10479-017-2593-1.
[105] United Nations Conference on Trade and Development. Review of maritime transport 2023. Tech. rep., United Nations Publications; 2023.
[106] Mauro F, Kana A. Digital twin for ship life-cycle: A critical systematic review. Ocean Eng 2023;269:113479. http://dx.doi.org/10.1016/j.oceaneng.2022.113479.